Journal of Medicinal Chemistry

Article

pubs.acs.org/jmc

Synthesis, Antimitotic and Antivascular Activity of 1-(3′,4′,5′-Trimethoxybenzoyl)-3-arylamino-5-amino-1,2,4-triazoles

Romeo Romagnoli,*[,†] Pier Giovanni Baraldi,*[,†] Maria Kimatrai Salvador,[†] Filippo Prencipe,[†] Valerio Bertolasi,[†] Michela Cancellieri,[§] Andrea Brancale,[§] Ernest Hamel,[⊥] Ignazio Castagliuolo,[∥] Francesca Consolaro,[‡] Elena Porcù,[‡] Giuseppe Basso,[‡] and Giampietro Viola*[,‡]

[†]Dipartimento di Scienze Chimiche e Farmaceutiche, Università di Ferrara, Ferrara, Italy

[‡]Dipartimento di Salute della Donna e del Bambino, Laboratorio di Oncoematologia, Università di Padova, Padova, Italy

[§]The Welsh School of Pharmacy and Pharmaceutical Sciences, Cardiff University, Cardiff, U.K.

[∥]Dipartimento di Medicina Molecolare, Università di Padova, Padova, Italy

[⊥]Screening Technologies Branch, Developmental Therapeutics Program, Division of Cancer Treatment and Diagnosis, Frederick Laboratory for Cancer Research, National Institutes of Health, Frederick, Maryland

Supporting Information

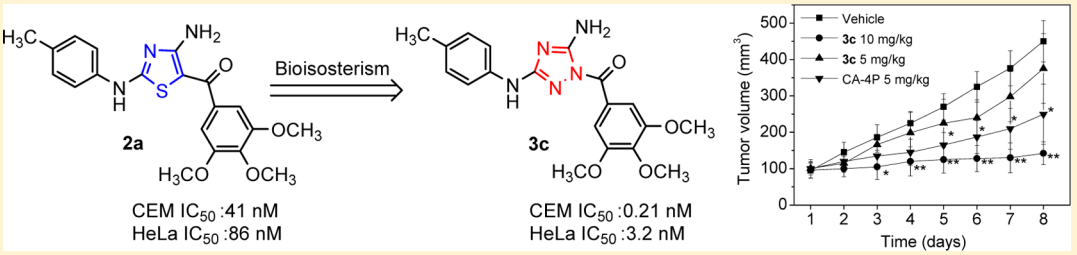

ABSTRACT: A new class of compounds that incorporated the structural motif of the 1-(3′,4′,5′-trimethoxtbenzoyl)-3-arylamino-5-amino-1,2,4-triazole molecular skeleton was synthesized and evaluated for their antiproliferative activity in vitro, interactions with tubulin, and cell cycle effects. The most active agent, **3c**, was evaluated for antitumor activity in vivo. Structure−activity relationships were elucidated with various substituents on the phenyl ring of the anilino moiety at the C-3 position of the 1,2,4-triazole ring. The best results for inhibition of cancer cell growth were obtained with the *p*-Me, *m*,*p*-diMe, and *p*-Et phenyl derivatives **3c**, **3e**, and **3f**, respectively, and overall, these compounds were more or less as active as CA-4. Their vascular disrupting activity was evaluated in HUVEC cells, with compound **3c** showing activity comparable with that of CA-4. Compound **3c** almost eliminated the growth of syngeneic hepatocellular carcinoma in Balb/c mice, suggesting that **3c** could be a new antimitotic agent with clinical potential.

INTRODUCTION

The cellular microtubule system, established by an equilibrium between the polymerization and depolymerization of $\alpha\beta$-tubulin heterodimers, is essential in a variety of cellular processes, including maintenance of cell shape, regulation of motility, intracellular transport of vesicles and organelles, and cell division.[1] Because of the latter function in eukaryotic cells, microtubules are a successful target for the development of numerous small natural and synthetic molecules that inhibit the formation of the mitotic spindle.[2−4] Among the naturally occurring antimicrotubule agents, one of the most active is the *cis*-stilbene combretastatin A-4 (CA-4, **1a**, Chart 1), isolated from the African cape bushwillow *Combretum caffrum*.[5] CA-4 inhibits tubulin assembly by strongly binding to the colchicine site on β-tubulin.[6] Its water-soluble prodrug, CA-4 disodium phosphate (CA-4P, **1b**),[7] is in advanced clinical trials,[8] and it was found to have potent activity in reducing tumor blood flow, thus acting as a vascular disrupting agent (VDA).[9]

Among the synthetic inhibitors of tubulin polymerization, we previously described a series of 2-arylamino-4-amino-5-(3′,4′,5′-trimethoxybenzoyl)thiazoles with general structure **2** that showed strong antiproliferative activity against a panel of five cancer cell lines.[10] These compounds also caused accumulation of HeLa cells in the G2/M phase of the cell cycle, as is typical for antimicrotubule agents. Derivatives **2a** (R_1 = H) and **2b** (R_1 = 4′-Me) were the most active as inhibitors of tumor cell growth, with IC_{50} values of 6−23 and 15−86 nM, respectively, in the five cell lines.

Ring bioisosterism is widely used as a rational approach for the discovery of new anticancer agents, especially for finding agents with optimal pharmacological properties.[11] Continuing our search strategy for novel and potent antimicrotubule agents, we have underway a pharmacophore exploration and optimization effort based on compounds with general formula

Received: May 29, 2014

   dx.doi.org/10.1021/jm5008193 | *J. Med. Chem.* XXXX, XXX, XXX−XXX

Chart 1. Inhibitors of Tubulin Polymerization

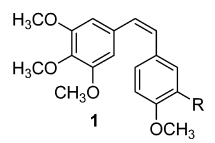

1

R=OH, Combretastatin A-4 (CA-4), **1a**
R=OPO_3Na_2, CA-4P, **1b**

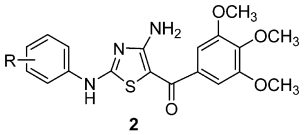

2

R=H, F, Cl, CH_3 and OCH_3
2a, R=H
2b, R=*p*-CH_3

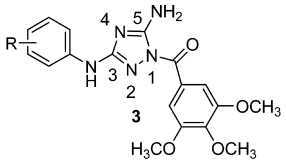

3

3a, R=H
3b, R=p-F
3c, R=p-CH_3
3d,R=m-CH_3
3e, R=m,p-$(CH_3)_2$
3f, R=p-C_2H_5
3g, R=p-$CH(CH_3)_2$
3h, R=p-$(CH_2)_3CH_3$
3i, R=p-OCH_3
3j, R=m-OCH_3
3k, R=m,p-$(OCH_3)_2$
3l, R=m,m',p-$(OCH_3)_3$
3m, R=p-OC_2H_5
3n, R=m,p-(OCH_2O)

Scheme 1[a]

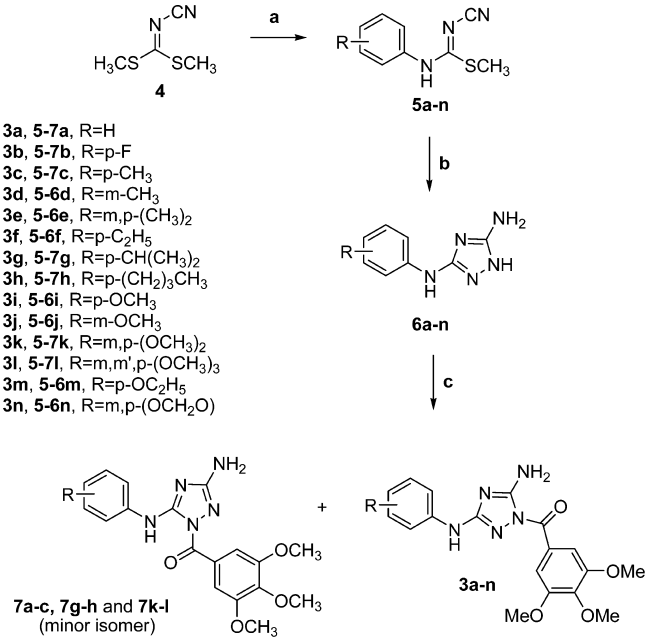

4

5a-n

3a, **5-7a**, R=H
3b, **5-7b**, R=p-F
3c, **5-7c**, R=p-CH_3
3d, **5-6d**, R=m-CH_3
3e, **5-6e**, R=m,p-$(CH_3)_2$
3f, **5-6f**, R=p-C_2H_5
3g, **5-7g**, R=p-$CH(CH_3)_2$
3h, **5-7h**, R=p-$(CH_2)_3CH_3$
3i, **5-6i**, R=p-OCH_3
3j, **5-6j**, R=m-OCH_3
3k, **5-7k**, R=m,p-$(OCH_3)_2$
3l, **5-7l**, R=m,m',p-$(OCH_3)_3$
3m, **5-6m**, R=p-OC_2H_5
3n, **5-6n**, R=m,p-(OCH_2O)

6a-n

7a-c, 7g-h and **7k-l** (minor isomer)

3a-n

[a]Reagents: (a) $ArNH_2$, *i*-PrOH, reflux; (b) $NH_2NH_2{\cdot}H_2O$, THF, reflux; (c) 3',4',5'-$(OMe)_3C_6H_2COCl$, pyridine, 0 °C.

2. Here we describe replacing the thiazole nucleus with the more electron-rich 1,2,4-triazole bioisosteric ring[12,13] to afford a new series of 1-(3′,4′,5′-trimethoxybenzoyl)-3-arylamino-5-amino 1,2,4-triazole analogues with general structure **3**. Our goal was to evaluate the steric and electronic effects of different substituents on the benzene portion of the arylamino moiety. Besides hydrogen (compound **3a**), the examined substituents included fluorine (**3b**) and electron donating alkyl and alkoxy groups (compounds **3c**−**h** and **3i**−**n**, respectively). Because it is well-known that the trimethoxyphenyl skeleton is the characteristic structural requirement to maximize activity in a large series of inhibitors of tubulin polymerization, such as colchicine, CA-4, and podophyllotoxin,[14] all newly prepared compounds **3a**−**n** retain the 3′,4′,5′-trimethoxybenzoyl group at the C-1 position of the 1,2,4-triazole ring. The newly synthesized derivatives were evaluated for their antiproliferative activity in a panel of human cancer cell lines for their antitubulin activity (including cell cycle and apoptotic effects) and their antivascular activity in HUVEC cells. Finally, the antitumor activity of **3c**, the most potent member of the group in the in vitro studies, was evaluated in vivo in a syngeneic hepatocellular carcinoma in Balb/c mice in comparison with CA-4P.

CHEMISTRY

Synthesis of compounds **3a**−**n** was accomplished using a three-step procedure described in Scheme 1. The condensation of dimethyl cyanodithioimidocarbonate **4**[15] with the appropriate substituted aniline resulted in the formation of imidates **5a**−**n**, which were cyclized into the corresponding 5-amino-1*H*-[1,2,4]-triazole derivatives **6a**−**n** in the presence of hydrazine hydrate in refluxing THF.[16] Treatment of **6a**−**n** with an equimolar quantity of 3′,4′,5′-trimethoxybenzoyl chloride resulted in the formation of compounds **3a**−**n** as the major regioisomers. In the synthesis of compounds **3a**−**c**, **3g**−**h**, and **3k**−**l**, the corresponding minor regioisomers **7a**−**c**, **7g**−**h**, and **7k**−**l**, respectively, were also isolated in pure form and low yields (5−12%).

X-ray crystallographic analysis of a representative compound (**3c**) was determined to confirm the regioselective aroylation at the less sterically hindered *N*-1 nitrogen of the 1,2,4-triazole ring. Single crystals of **3c** were grown by slow evaporation from *i*-PrOH−MeOH solution, and the ORTEP view of compound **3c** is shown in Figure 1. The molecule displays an intramolecular N4−H···O1 hydrogen bond having N4···O1 and H···O1 distances of 2.773(3) and 2.12(3) Å, respectively, and an N4−H···O1 angle of 128(2)°.

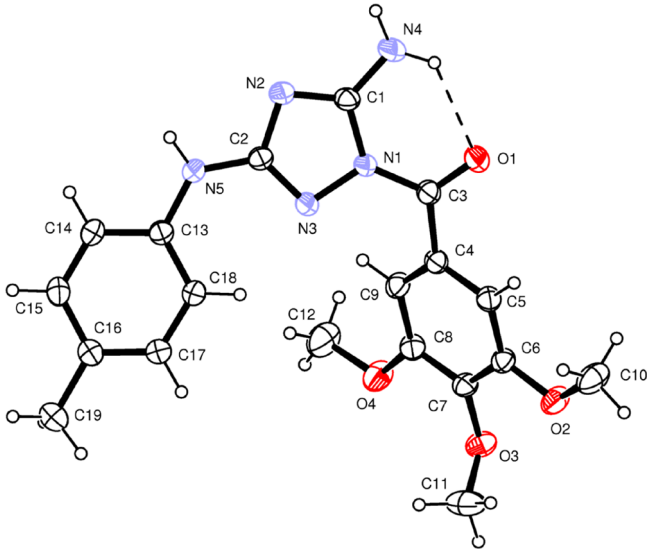

Figure 1. ORTEP view of compound **3c** displaying the thermal ellipsoids at 30% probability.

dx.doi.org/10.1021/jm5008193 | *J. Med. Chem.* XXXX, XXX, XXX−XXX

Table 1. In Vitro Cell Growth Inhibitory Effects of Compounds 3a−n and CA-4 (1)

	IC_{50}[a] (nM)						
compd	Jurkat	CCRF-CEM	SEM	HeLa	HT-29	A549	MCF-7
3a	1200 ± 270	1000 ± 90	1200 ± 190	>10 000	6200 ± 1200	>10 000	500 ± 240
3b	1900 ± 400	2200 ± 400	2400 ± 210	410 ± 70	2000 ± 700	3800 ± 160	370 ± 30
3c	0.81 ± 0.03	0.21 ± 0.04	0.51 ± 0.10	3.2 ± 1.3	0.82 ± 0.10	0.51 ± 0.22	1.0 ± 0.61
3d	42 ± 16	330 ± 60	30 ± 10	440 ± 50	460 ± 80	870 ± 30	15 ± 3.2
3e	2.0 ± 0.11	0.81 ± 0.10	0.40 ± 0.11	2.0 ± 0.82	3.0 ± 0.91	1.0 ± 0.82	4.0 ± 0.21
3f	1.0 ± 0.09	3.0 ± 0.09	0.81 ± 0.21	6.0 ± 1.0	0.21 ± 0.08	0.92 ± 0.51	5.0 ± 1.0
3g	520 ± 40	1800 ± 90	500 ± 10	130 ± 28	800 ± 100	550 ± 70	510 ± 70
3h	>10 000	>10 000	>10 000	>10 000	>10 000	>10 000	5200 ± 110
3i	51 ± 10	1000 ± 200	44 ± 16	120 ± 30	480 ± 15	2400 ± 100	260 ± 80
3j	7.2 ± 2.0	120 ± 30	1.0 ± 0.4	30 ± 1.2	700 ± 32	54 ± 4.3	11 ± 4.2
3k	>10 000	9000 ± 330	>10 000	>10 000	>10 000	>10 000	>10 000
3l	>10 000	>10 000	>10 000	>10 000	>10 000	>10 000	>10 000
3m	2500 ± 220	2000 ± 100	1900 ± 170	2100 ± 800	3700 ± 400	6200 ± 540	34 ± 18
3n	24 ± 7.2	40 ± 3.3	30 ± 6	930 ± 54	60 ± 10	150 ± 50	19 ± 5.2
CA-4	5 ± 0.6	12 ± 2.5	5 ± 0.1	4 ± 0.1	3100 ± 100	180 ± 50	370 ± 100

[a] IC_{50}= compound concentration required to inhibit tumor cell proliferation by 50%. Data are expressed as the mean ± SE from the dose−response curves of at least three independent experiments carried out in triplicate.

BIOLOGICAL RESULTS AND DISCUSSION

In Vitro Antiproliferative Activities. Table 1 summarizes the antiproliferative effects of 1-(3′,4′,5′-trimethoxybenzoyl)-3-anilino-5-amino 1,2,4-triazoles **3a−n** against a panel of seven human cancer cell line, using CA-4 (**1**) as the reference compound. The 1-(3′,4′,5′-Trimethoxybenzoyl)-3-amino-5-anilino 1,2,4-triazole isomers **7a−c**, **7g−h**, and **7k−l** were also evaluated for their activities, but because they were all inactive (IC_{50} > 10 μM), the data are not shown in Table 1. Three of the synthesized compounds, corresponding to the *p*-Me, *m*,*p*-di-Me, and *p*-Et phenyl analogues **3c**, **3e**, and **3f**, respectively, were significantly more active than the rest of derivatives, with IC_{50} values of 0.21−3.2, 0.4−4.0, and 0.21−6.0 nM, respectively, in the seven cell lines, as compared with 4−3100 nM for CA-4. With average IC_{50} values of 1.0, 1.9, and 2.4 nM for **3c**, **3e**, and **3f**, respectively, **3c** appears to be the most active compound in the series (for CA-4, the average value was 525 nM or, excluding the HT-29 cell line from the average, 96 nM). Thus, these three compounds are substantially more active than CA-4, and they are also more potent than their previously described isosteres **2a** and **2b**.[11] In addition to these highly potent three derivatives, the *m*-OMe and *m*,*p*-methylenedioxy phenyl derivatives **3j** and **3n**, respectively, were more active than CA-4 against HT-29, A549 and MCF-7 cells. In short, the data shown in Table 1 indicate the importance of substituents and their relative position on the phenyl ring of the arylamino moiety at the C-3 position of the 1,2,4-triazole skeleton for activity and selectivity against different cancer cell lines.

The unsubstituted anilino derivative **3a** was weakly active (IC_{50} > 0.5 μM), and the introduction of a weak electron-releasing fluorine atom at the *para*-position of the phenyl (compound **3b**) had the opposite effect, with slightly improved antiproliferative activity with respect to **3a** against HeLa, HT-29, A549, and MCF-7 cells, while the activity was reduced against Jurkat, CCRF-CEM, and SEM cells.

We found that the small methyl group at the *para*-position of the phenyl ring, to furnish derivative **3c**, improved significantly antiproliferative activity relative to **3a**. Moving the methyl group from the *para*- to the *meta*-position, to furnish isomer derivative **3d**, reduced antiproliferative activity from 1 to 3 orders of magnitude, with double-digit nanomolar activity against Jurkat, SEM, and MCF-7 cells. Because the *para*-toluidino moiety of **3c** was favorable for potency, it is important to point out that the introduction of an additional methyl group at the *meta*-position, resulting in the *meta*,*para*-dimethyl derivative **3e**, produced a 2−4-fold reduction in antiproliferative activity against five of the six cancer cell lines, while **3c** and **3e** were equipotent against SEM and HeLa cells.

The *para*-ethyl homologue **3f** was 2−15-fold less active than methyl counterpart **3c** against four of the seven cancer cell lines, with a minimal difference between the two compounds in the Jurkat and SEM cells, while **3f** was 4-fold more potent than **3c** against HT-29 cells. Replacing the *para*-ethyl group with branched (*i*-Pr) or larger (*n*-butyl) moieties (compounds **3g** and **3h**, respectively) was detrimental for activity in all cell lines, suggesting that an increase in steric bulk at this position caused a decrease in potency.

The number and position of methoxy substituents on the phenyl ring (compounds **3i−l**) had a major influence on antiproliferative activity. Replacement of the methyl moiety with a more electron-releasing methoxy group at the *para*-position of the phenyl ring (compound **3i**) decreased antiproliferative activity by 100-fold compared with **3c**, indicating that the methyl and methoxy groups are not bioequivalent at the *para*-position of the phenyl ring. The contribution of methyl or methoxy groups on the phenyl ring to activity (**3c** vs **3d** and **3i** vs **3j**, respectively) was position dependent, with opposite effects. While for the methyl group, as previously observed, the *para*-derivative **3c** was considerably more potent than *meta*-isomer **3d**, an opposite effect was observed for the two methoxy isomers **3i** and **3j**, with the *meta*-isomer **3j** from 4- to 44-fold more potent than the *para*-isomer **3i** in six of the seven cancer cell lines, the exception being the HT-29 cells. Either two or three methoxy substituents (derivatives **3k** and **3l**, respectively) caused substantial loss in antiproliferative activity relative to **3i** and **3j**, suggesting that steric factors account for the loss of activity observed with these two compounds. With the exception of the MCF-7 cells, the *para*-ethoxy derivative **3m** was 2−50-fold less potent than its methoxy counterpart **3m**. The 3′,4′-methylenedioxy derivative **3n**, with IC_{50} values in the double-digit nanomolar range in five

dx.doi.org/10.1021/jm5008193 | J. Med. Chem. XXXX, XXX, XXX−XXX

of the seven cancer cell lines, showed an antiproliferative activity intermediate between those of *para*- and *meta*-methoxy analogues **3i** and **3j**, respectively.

Evaluation of Cytotoxicity in Human Noncancer Cells. To obtain a preliminary indication of the cytotoxic potential of these derivatives for normal human cells, two of the most active compounds (**3c** and **3f**) were assayed in vitro against peripheral blood lymphocytes (PBL) from healthy donors (Table 2). Both compounds were practically ineffective in quiescent lymphocytes, with an IC_{50} of about 30 μM. In the presence of the mitogenic stimulus phytohematoagglutinin (PHA), the IC_{50} decreased to about 8 μM for both compounds, a value that is thousands of times higher than those observed against the lymphoblastic cell lines Jurkat and CCRF-CEM. Furthermore, compound **3c** was also evaluated in human umbilical vein endothelial cells (HUVECs), and again the IC_{50} value was negligible compared with those found in the panel of cancer cell lines. Altogether, these data suggest that these compounds may have cancer cell selective antiproliferative properties.

Table 2. Cytotoxicity of 3c and 3f in Human Noncancer Cells[a]

	IC_{50} (μM)[b]	
cell line	3c	3f
$PBL_{resting}$[c]	31.2 ± 8.7	34.0 ± 11.7
PBL_{PHA}[d]	8.5 ± 2.6	8.8 ± 2.7
HUVEC	11.9 ± 3.8	nd

[a]Values are the mean ± SEM for three separate experiments. nd: not determined. [b]Compound concentration required to reduce cell growth inhibition by 50%. [c]PBL not stimulated with PHA. [d]PBL stimulated with PHA.

Effect of Compound 3c on Drug-Resistant Cell Lines. Drug resistance has become a serious problem in cancer chemotherapy.[17,18] One of the common mechanisms of resistance so far identified both in preclinical and clinical studies involves the overexpression of a cellular membrane protein called P-glycoprotein (P-gp) that mediates the efflux of various structurally unrelated drugs.[17,18] We evaluated sensitivity of compound **3c** in two multidrug-resistant cell lines, one derived from a colon carcinoma ($Lovo^{Doxo}$)[19] the other derived from a lymphoblastic leukemia ($CEM^{Vbl\text{-}100}$).[20] Both these lines express high levels of the P-gp.[19,20] As shown in Table 3, compound **3c** was almost equally potent toward cells resistant to doxorubicin or vinblastine showing a resistance index (RI), which is the ratio between GI_{50} values of resistant cells and sensitive cells, of 1.2 and 5.7 respectively, while doxorubicin in $LoVo^{Doxo}$ and vinblastine in CEM^{Vbl100} showed a high RI of 118 and 193, respectively. Altogether, these results suggest that this compound might be useful in the treatment of drug refractory tumors.

Table 3. In Vitro Cell Growth Inhibitory Effects of Compound 3c on Drug Resistant Cell Lines

	IC_{50}[a] (nM)		
compd	LoVo	$LoVo^{Doxo}$	resistance ratio[b]
3c	0.9 ± 0.1	1.1 ± 0.5	1.2
doxorubicin	95.6 ± 43.2	11296 ± 356	118
	CEM	CEM^{Vbl100}	resistance ratio[b]
3c	0.21 ± 0.4	1.2 ± 0.5	5.7
vinblastine	1.0 ± 0.3	193 ± 39	193

[a]IC_{50} = compound concentration required to inhibit tumor cell proliferation by 50%. Data are presented as the mean ± SE from the dose–response curves of two independent experiments performed in triplicate. [b]The values express the ratio between IC_{50} determined in resistant and nonresistant cell lines.

Inhibition of Tubulin Polymerization and Colchicine Binding. A subset of the compounds (**3c–g**, **3i–j** and **3n**) were evaluated for their in vitro inhibition of tubulin polymerization in comparison with CA-4. The same compounds were also examined for inhibitory effects on the binding of [^{3}H]colchicine to tubulin (Table 4). In the assembly assay, with 10 μM tubulin, compound **3c** was highly potent, yielding an IC_{50} of 0.75 μM, almost twice as active as CA-4. Derivatives **3e** and **3f** had IC_{50} values of 1.2 and 1.4 μM, comparable to the value obtained with CA-4. Compounds **3d**, **3i–j**, and **3n** were less active as inhibitors of tubulin polymerization, with IC_{50} values of 1.8, 3.7, 2.5, and 2.0 μM, respectively, while **3g** was, relatively speaking, almost inactive. The order of inhibitory effects on tubulin assembly was **3c** > **3e** = CA-4 > **3f** > **3d** > **3n** > **3j** > **3i** ≫ **3g**. This order of activity as inhibitors of tubulin assembly correlates well with their order of activity as antiproliferative agents against Jurkat, CCRF-CEM, SEM, and HeLa cells.

Table 4. Inhibition of Tubulin Polymerization and Colchicine Binding by Compounds 1a, 3c–g, 3i–j, and 3n

compd	tubulin assembly[a] IC_{50} ± SD (μM)	colchicine binding[b] % ± SD
3c	0.75 ± 0.1	92 ± 2
3d	1.8 ± 0.0	67 ± 1
3e	1.2 ± 0.0	83 ± 1
3f	1.4 ± 0.0	80 ± 2
3g	13 ± 0.7	nd[c]
3i	3.7 ± 0.4	48 ± 2
3j	2.5 ± 0.0	70 ± 0.9
3n	2.0 ± 0.0	51 ± 0.3
1a	1.2 ± 0.1	98 ± 0.5

[a]Inhibition of tubulin polymerization. Tubulin was at 10 μM. [b]Inhibition of [^{3}H]colchicine binding. Tubulin, colchicine and tested compound were at 1, 5, and 5 μM, respectively. [c]nd: not determined

In the competition assay, compound **3c** was again the most active derivative, inhibiting colchicine binding by 92% versus 98% for CA-4. In the experiments summarized in Table 4, the concentration of tubulin was 1.0 μM, while that of both the inhibitors and [^{3}H]colchicine was 5.0 μM. Inhibition of colchicine binding by compounds **3e** and **3f** was lower, with 83% and 80% inhibition occurring with these agents. With the exception of compounds **3j** and **3n**, a good correlation was observed between antiproliferative activities, inhibition tubulin polymerization, and inhibition of colchicine binding.

To further investigate if the new derivatives interfered with the microtubule network, we examined the effects of **3c** on HeLa cells by immunofluorescence microscopy. Following a 24 h treatment with **3c** at 50, 100, and 250 nM, the microtubule network was substantially modified in comparison with the untreated cells (Figure S1, Supporting Information). Altogether, these results are consistent with the conclusion that the antiproliferative activity of these compounds derived from an interaction with the colchicine site of tubulin, and this ultimately results in interference with microtubule assembly.

dx.doi.org/10.1021/jm5008193 | J. Med. Chem. XXXX, XXX, XXX–XXX

Molecular Modeling. To rationalize the experimental data observed for **3a**–**n**, we performed a series of molecular docking simulations of these compounds in the colchicine site of tubulin. The proposed binding mode for **3c** is very similar to the one presented by the co-crystallized DAMA–colchicine (Figure 2A). In particular, it is possible to observe how the

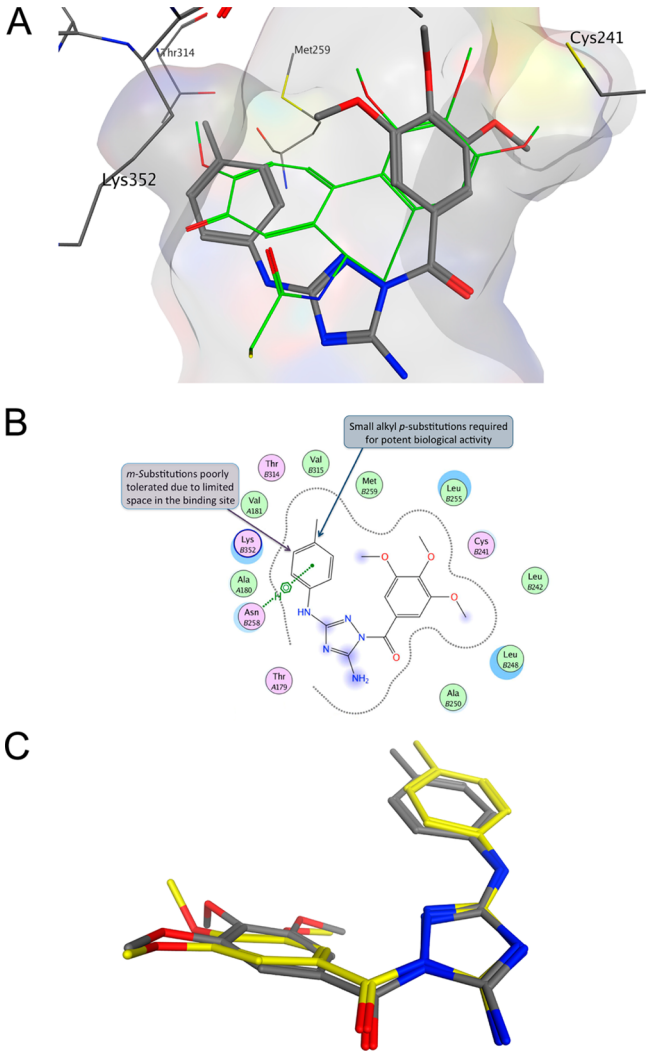

Figure 2. (A) Proposed binding for **3c** (in gray) in the colchicine site. Co-crystallized DAMA–colchicine is shown in green. (B) Representation of the binding mode of **3c** in the colchicine site, with a summary of the SARs observed for the reported series of compounds. (C) Superposition of the conformation obtained from the docking simulations (in gray) and the crystal structure (in yellow) of **3c**.

trimethoxyphenyl ring is in proximity of Cys241, while the phenyl ring occupies a hydrophobic region deep in the binding site, establishing a series of interactions with Met259, Thr314, and Lys352. Indeed, this subpocket is relatively small and, while the methyl substituent on the phenyl ring of **3c** is able to fit in properly, larger groups, such as the isopropyl (**3g**) or the *n*-butyl (**3h**), cannot be accommodated into it. In these cases, the docking simulations are not able to generate a reasonable binding pose. The docking results are in accordance with the experimental data, and they provide a possible structural justification of the SARs observed (Figure 2B). Finally, it is interesting to note that the **3c** binding conformation generated in the docking simulation is very similar to the conformation of the structure obtained experimentally by X-ray crystallography (Figure 2C).

Analysis of 3-Arylamino 1,2,4-Triazole Derivatives for Effects on the Cell Cycle. The effects of a 24 h treatment with different concentrations of **3c** on cell cycle progression in HeLa and Jurkat cells were determined by flow cytometry (Figure 3A,B). The compound caused a significant G2/M arrest in a

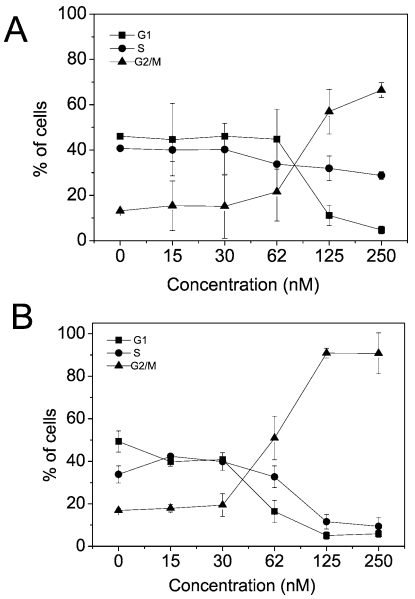

Figure 3. Percentage of cells in each phase of the cell cycle in HeLa (A) and Jurkat cells (B) treated with **3c** at the indicated concentrations for 24 h. Cells were fixed and labeled with PI and analyzed by flow cytometry as described in the Experimental Section. Data are represented as mean ± SEM of three independent experiments.

concentration-dependent manner in the cell lines tested, with a rise in G2/M cells occurring at a concentration as low as 60 nM, while, at higher concentrations, more than 70% of the cells were arrested in G2/M. The cell cycle arrest in the G2/M phase was accompanied by a corresponding reduction in cells in the other phases of the cell cycle. In particular, the G1 phase decreased in both cell lines, whereas S phase reduction was mainly evident in Jurkat cells.

We next studied the association between **3c**-induced G2/M arrest and alterations in expression of proteins that regulate cell division. As shown in Figure 4 in HeLa cells, a 24 h treatment with **3c** at concentrations lower than 100 nM caused no significant variation in cyclin B expression, which, in association with cdc2, controls both entry into and exit from mitosis,[21,22] while at 100 and 250 nM, we observed a clear increase in the cyclin B1 band. After a 48 h treatment, cyclin B1 expression decreased. More importantly, p-cdc2^{Tyr15} expression decreased after either 24 or 48 h of treatment. However, no major changes in the expression of phosphatase cdc25c were observed. These results indicate that arrest at G2/M induced by **3c** is caused by an immediate block of cyclin B1 activity, followed by its accumulation, leading to a persistent and marked decrease of p-cdc2^{Tyr15} more detectable at the highest concentrations (100–250 nM) examined.

In addition to the analysis of proteins that control cell cycle checkpoints, we also examined the expression of the tumor suppressor p53 after treatment of Hela cells with **3c**. It is well-known that prolonged mitotic arrest induces DNA damage and,

dx.doi.org/10.1021/jm5008193 | J. Med. Chem. XXXX, XXX, XXX–XXX

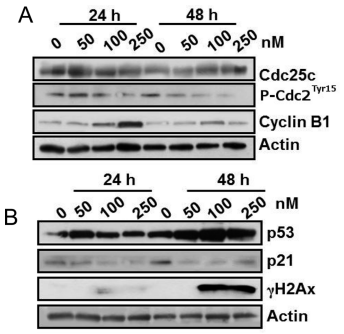

Figure 4. Effects of **3c** on G2/M regulatory proteins (A) and on p53, p21, and γH2AX expression (B). HeLa cells were treated for 24 or 48 h with the indicated concentration of **3c**. The cells were harvested and lysed for the detection of cyclin B1, p-cdc2^{Tyr15}, and cdc25C (A) or p53, p21, and γH2AX expression (B) by Western blot analysis. To confirm equal protein loading, each membrane was stripped and reprobed with anti-β-actin antibody.

consequently, p53 up-regulation.[23,24] As shown in Figure 4B, we detected in a concentration-dependent manner an increase in p53 expression that is particularly evident after 48 h of treatment. At the same time, we also observed a marked increase in the expression of phosphorylated histone γH2A.X, which is an early sensitive indicator of DNA damage.[25] Interestingly, the expression of the cyclin-dependent kinase inhibitor p21, which was previously demonstrated to have an antiapoptotic role,[26] decreased both after 24 and 48 h of treatment.

Compound ***3c*** *Induces Apoptosis.* To characterize the mode of cell death induced by **3c**, a biparametric cytofluorimetric analysis was performed using propidium iodide (PI), which stains DNA and enters only dead cells, and fluorescent immunolabeling of the protein annexin-V, which binds to phosphatidylserine (PS) in a highly selective manner.[27] Dual staining for annexin-V and with PI permits discrimination between live cells (annexin-V$^-$/PI$^-$), early apoptotic cells (annexin-V$^+$/PI$^-$), late apoptotic cells (annexin-V$^+$/PI$^+$), and necrotic cells (annexin-V$^-$/PI$^+$). As shown in Figure 5, both HeLa (panel A) and Jurkat cells (panel B) treated with the two compounds for 24 h showed an accumulation of annexin-V positive cells that further increased after 48 h in comparison with the untreated cells. Analogous results were also obtained for compound **3e** (see Figure S2, Supporting Information).

Compound ***3c*** *Induces Caspase-Dependent Apoptosis.* We then analyzed by Western blot which proteins are involved on the triggered apoptotic pathway upon treatment with **3c**. HeLa cells were treated with different concentrations of **3c** for 24 or 48 h (Figure 6). Interestingly, **3c** induced activation of the initiator caspase-9 in a time and concentration-dependent manner. We observed also an activation of the effector caspase-3 and cleavage of its substrate PARP. Furthermore, the antiapoptotic protein Bcl-2 was decreased by treatment with **3c** in a time dependent manner, while the expression of a pro-apoptotic protein, Bax, was slightly increased only at 250 nM and at 48 h.

Derivative ***3c*** *has Antivascular Effects in Vitro.* Tumor growth requires an oxygen supply, so the tumor microenvironment stimulates the development of additional blood vessels.[28] Recent antitumor strategies are based on the use of chemotherapeutics with antiangiogenic or antivascular drugs in order to increase the efficacy of the treatment.[29] Many

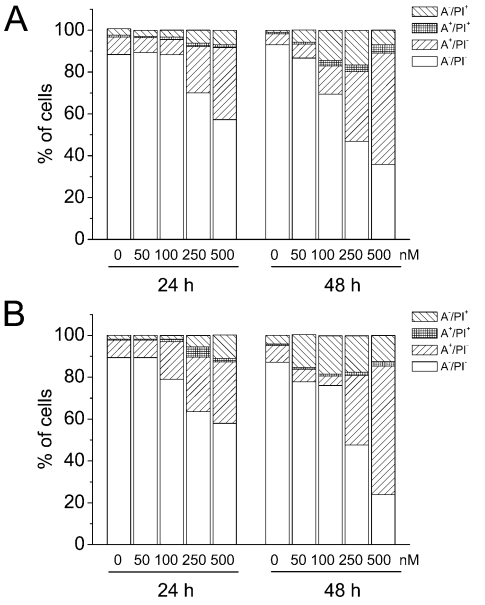

Figure 5. Flow cytometric analysis of apoptotic cells after treatment of HeLa cells (A) or Jurkat cells (B) with **3c** at the indicated concentrations after incubation for 24 or 48 h. The cells were harvested and labeled with annexin-V-FITC and PI and analyzed by flow cytometry. Data are represented as mean ± SEM of three independent experiments.

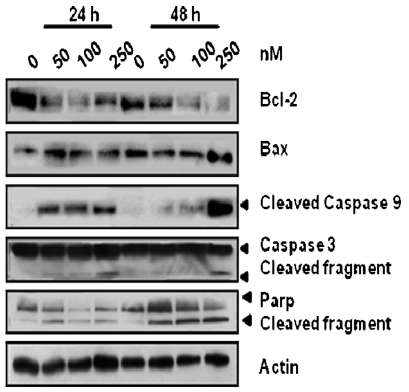

Figure 6. Western blot analysis of caspase-3, cleaved caspase-9, PARP Bcl-2, and Bax after treatment of HeLa cells with **3c** at the indicated concentrations and for the indicated times. To confirm equal protein loading, each membrane was stripped and reprobed with anti-β-actin antibody.

tubulin binding agents show antivascular effects against tumor endothelium,[30] including CA-4, and for that reason we evaluated **3c** for effects on endothelial cells in vitro. We used human umbilical vein endothelial cells (HUVECs) as a model for angiogenesis/vasculogenesis processes in vitro. Endothelial cell migration to the tumor site is one of the described mechanisms of angiogenesis.[31] Inhibiting this mechanism could be a strategy to arrest the development of tumor vasculature. We evaluated cell motility by scratching a HUVEC monolayer and monitoring the ability of cells to reclose the wound. As shown in Figure 7A, **3c** is very efficient in arresting cell motility. The effect is statistically significant after a 24 h incubation, at all the tested concentrations (5, 10, 25 nM), while after 6 h, **3c** significantly inhibited cell motility at 10 and 25 nM, with a dose−response relationship observed (Figure 7B).

dx.doi.org/10.1021/jm5008193 | J. Med. Chem. XXXX, XXX, XXX−XXX

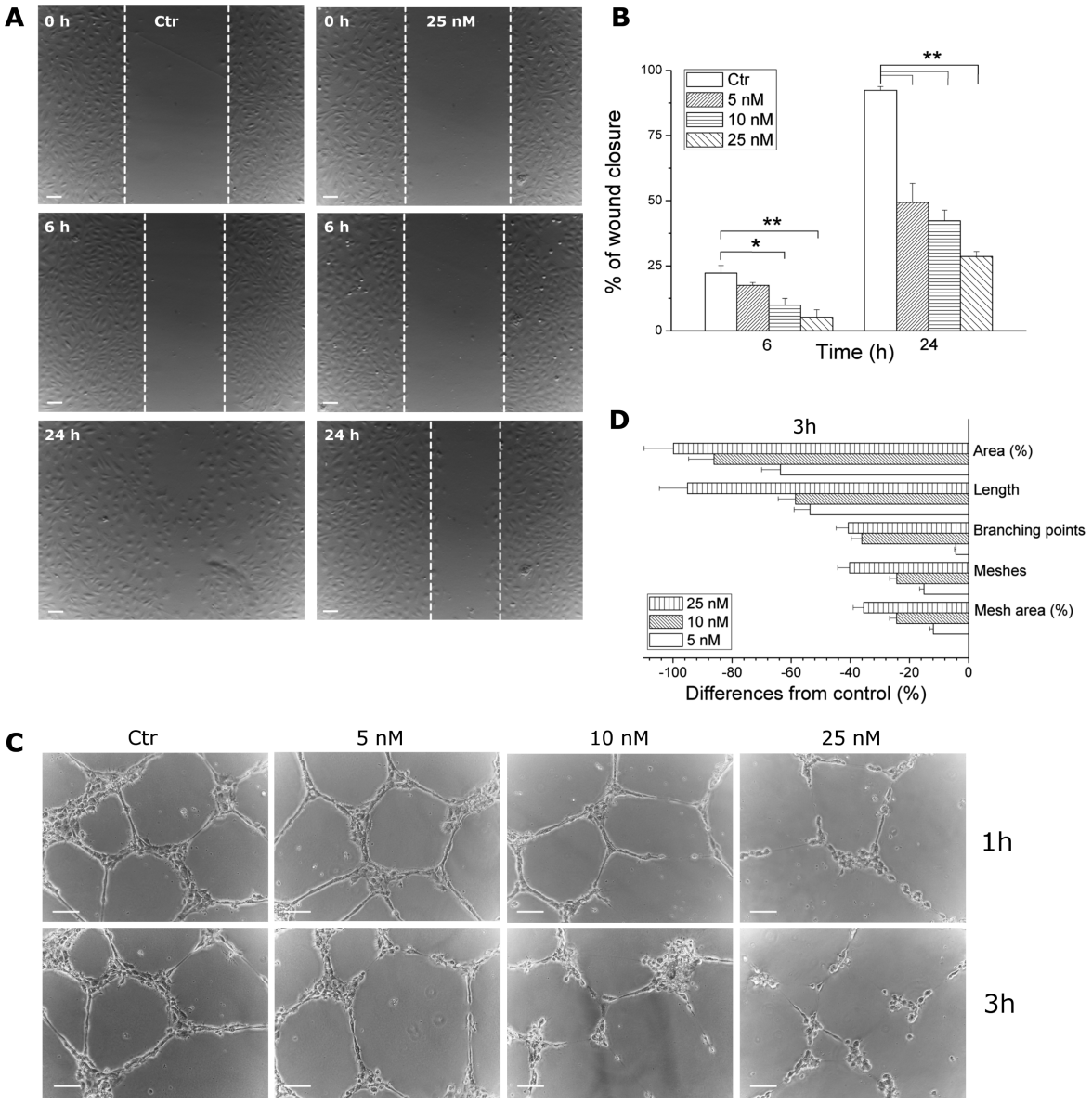

Figure 7. Compound **3c** has antivascular activity in vitro. (A) Confluent HUVECs in a monolayer were wounded, and cells treated with different concentrations of **3c** and at different times were photographed, 7× magnification; bar = 100 μm. The dotted lines define the areas lacking cells. (B) The graph shows the quantitative effect of **3c**. Migration was quantified by measuring the gap closure at the indicated times as shown in A. Data are represented as mean ± SEM of three independent experiments. *$p < 0.05$, **$p < 0.01$ vs control. (C) Inhibition of endothelial cell capillary-like tubule formation by **3c**. Tubule formation on Matrigel was carried out as described in the Experimental Section. Representative pictures (10× magnification; bar = 100 μm) of preformed capillary-like tubules treated with increasing concentrations of **3c** for 1 or 3 h. (D) Quantitative analysis of the effects of **3c** on the dimensional and topological parameters of the preformed capillary-like tubule networks after a 3 h treatment. Data were represented as mean ± SEM of three independent experiments. *$p < 0.05$, **$p < 0.01$ vs. control.

To support the antivascular activity of **3c**, we evaluated the ability of the compound to disrupt the "tubule-like" structures, formed by HUVECs seeded on Matrigel. Matrigel is an extracellular matrix, rich in pro-angiogenic factors that stimulate single endothelial cells to assume an extended shape. The overall effect results in a reticulum similar to a capillary network.

As shown in Figure 7C, after a 1 h incubation, 25 nM **3c** visibly disrupted the network of HUVECs, as compared with the control. After 3 h, all the tested concentrations were effective in altering the tubule-like structures. An image analysis[32] was performed to obtain a quantitative measurement of the total length of the tubules, the area and the number of meshes, the percent of area covered by HUVECs, and the number of branching points (Figure 7D) after a 3 h treatment.

The results indicate that the effects on endothelial cells induced by **3c** are similar to those observed after CA-4 treatment, in the same experimental conditions, carried out by our group.[33]

*Evaluation of Antitumor Activity of Compound **3c** in Vivo.* To evaluate the in vivo antitumor activity of **3c**, a syngeneic hepatocellular carcinoma model in mice was used.[34] Tumors were established by subcutaneous injection of BNL 1ME A.7R.1 cells into the backs of Balb/c mice. In preliminary experiments in vitro, we determined that both compound **3c** and CA-4, used as a reference compound, showed similar,

dx.doi.org/10.1021/jm5008193 | J. Med. Chem. XXXX, XXX, XXX−XXX

potent cytotoxic activity (**3c** IC_{50} = 3.4 ± 1.1 nM; CA-4 IC_{50} = 1.1 ± 0.5 nM) against BNL 1ME A.7R.1 cells. Once the allografts reached a measurable size (about 100 mm^3), 20 mice were randomly assigned to one of four groups. In two of the groups, compound **3c** was injected intraperitoneally at doses of 5 and 10 mg/kg, respectively. In a third group, CA-4P was injected at 5 mg/kg, while the fourth group was used as a control. As depicted in Figure 8A, compound **3c** caused a

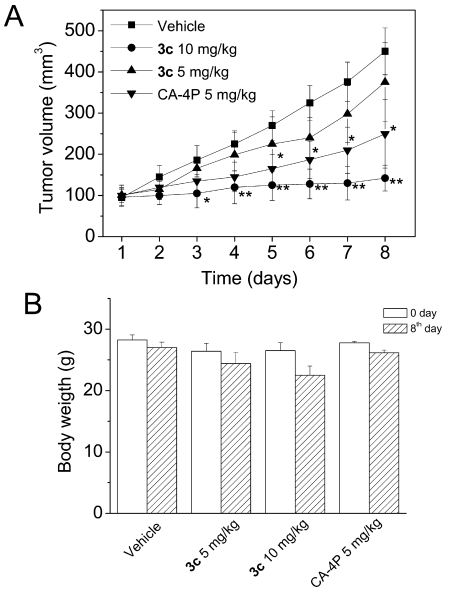

Figure 8. Inhibition of mouse allograft tumor growth in vivo by compound **3c**. (A) Male mice were injected subcutaneously in their dorsal region with 10^7 BNL 1MEA.7R.1 cells, a syngeneic hepatocellular carcinoma cell line. Tumor-bearing mice were administered the vehicle, as control, or the indicated doses of **3c** or CA-4P as reference compound at the concentration of 5 mg/kg. Daily injections were given intraperitoneally starting on day 1. The figure shows the average measured tumor volumes (A) and body weights of the mice (B) recorded at the beginning and at the end of the treatments. Data are presented as mean ± SEM of tumor volume and body weight at each time point for five animals per group. *$p < 0.05$, **$p < 0.01$ vs. control.

significant reduction in tumor growth, as compared with administration of vehicle, at 10 but not 5 mg/kg. The effect of 5 mg/kg of CA-4P was not as great as that of 10 mg/kg of **3c**, but the CA-4P effect was still significant relative to the control. During the treatment period, only a small decrease in body weight occurred in the **3c**-treated animals (Figure 8B).

CONCLUSIONS

The bioisosteric equivalence between thiazole and 1,2,4-triazole prompted us to synthesize a series of 1-(3′,4′,5′-trimethoxybenzoyl)-3-arylamino-5-amino 1,2,4-triazole derivatives with general formula **3**, in which the 1,2,4-triazole ring replaced the thiazole system of previously published analogues with general structure **2**. The substitution pattern on the phenyl of the arylamino moiety had variable effects.

Compound **3c**, bearing a *p*-toluidino moiety at the C-3 position of 1,2,4-triazole ring, its *p*-ethyl homologue **3f**, and the *m*,*p*-dimethyl analogue **3e** exhibited the greatest antiproliferative activity among the tested compounds, with IC_{50} values of 0.21−3.2, 0.21−6.0, and 0.4−4.0 nM, respectively. These results were superior or comparable with those of the reference compound CA-4 against all cancer cell lines. The *para*-position tolerates small substituents, such as methyl (**3c**) or ethyl (**3f**) groups, while the inactivity of *i*-Pr or *n*-Bu derivatives **3g** and **3h**, respectively, indicates that bulky substituents were detrimental for activity. Placing the methyl group in the *meta*-position (**3d**) led to a dramatic drop in potency as compared with the *para*-isomer **3c**, even though we observed excellent activity with the *meta*,*para*-dimethyl derivative **3e**. Compound **3c** was the most potent inhibitor of tubulin polymerization and of colchicine binding (IC_{50} = 0.75 μM for assembly, 92% inhibition of the binding of 5 μM colchicine), and the antiproliferative activity of **3c**, in terms of IC_{50s}, ranged from 0.21 to 3.2 nM in the seven cell tumor lines examined, values lower than that of previously published isosteric analogues.[11] In addition, in preliminary experiment **3c** had low toxicity in nontumoral cells and is active also in drug-resistant cell lines. Although **3c** was almost twice as active as CA-4 as an inhibitor of tubulin polymerization, these two compounds showed similar activity as inhibitors of colchicine binding. Moreover, in a detailed series of biological assays, we clearly demonstrated that **3c** induced caspase-dependent apoptosis and late DNA damage and p53 induction. Compound **3c**, in addition to its ability to inhibit tubulin polymerization, efficiently targeted endothelial cells, acting as a VDA. More importantly, in vivo experiments showed that this compound was able to significantly reduce the growth of a syngeneic tumor model in mice, indicating that it is a very promising anticancer compound that warrants further evaluation for its potential clinical use.

EXPERIMENTAL SECTION

Chemistry: Materials and Methods. ^1H and ^{13}C NMR data were obtained with a Varian VXR 200 spectrometer and a Varian Mercury Plus 400 spectrometer, respectively. Peak positions are given in parts per million (δ) downfield, and *J* values are given in hertz. Positive-ion electrospray ionization (ESI) mass spectra were recorded on a double-focusing Finnigan MAT 95 instrument with BE geometry. Melting points (mp) were determined on a Buchi-Tottoli apparatus and are uncorrected. The purity of tested compounds was determined by combustion elemental analyses conducted by the Microanalytical Laboratory of the Chemistry Department of the University of Ferrara with a Yanagimoto MT-5 CHN recorder elemental analyzer. All tested compounds yielded data consistent with a purity of at least 95% as compared with the theoretical values. All reactions were carried out under an inert atmosphere of dry nitrogen unless otherwise indicated. TLC was carried out using glass plates coated with silica gel 60 F_{254} by Merck, and compounds were visualized by UV detection or with aqueous $KMnO_4$. Flash column chromatography was performed using 230−400 mesh silica gel and the indicated solvent system. Organic solutions were dried over anhydrous Na_2SO_4. Solvents and reagents that are commercially available were purchased from Aldrich (Sigma-Aldrich) or Alfa Aesar (Johnson Matthey Company) and were used without further purification unless otherwise noted.

General Procedure A for the Synthesis of Compounds 5a−n. To a solution of the appropriate aniline derivative (3 mmol, 1 equiv) in 2-propanol (10 mL) was added dimethyl cyanodithioimidocarbonate **4** (439 mg, 3 mmol), and the mixture was refluxed for 16 h. After this time, the solvent was removed under reduced pressure, and the resulting residue was suspended in ethyl ether (10 mL) and filtered to furnish the final compound **5a−n** used for the next reaction without any purification.

*(Z)-Methyl N′-Cyano-N-phenylcarbamimidothioate (**5a**).* Synthesized according to method A, derivative **5a** was obtained as a white solid (yield 71%); mp 192−193 °C. ^1H NMR ($CDCl_3$) δ: 2.46 (s, 3H), 7.38 (m, 5H), 7.92 (bs, 1H). MS (ESI): $[M + 1]^+$ = 192.3.

dx.doi.org/10.1021/jm5008193 | J. Med. Chem. XXXX, XXX, XXX−XXX

*(Z)-Methyl N′-Cyano-N-(4-fluorophenyl)carbamimidothioate (**5b**).* Synthesized according to method A, compound **5b** was obtained as a gray solid (yield 78%); mp 216−218 °C. ^{1}H NMR ($CDCl_3$) δ: 2.45 (s, 3H), 7.12 (t, J = 8.0 Hz, 2H), 7.29 (m, 2H), 7.94 (bs, 1H). MS (ESI): $[M + 1]^+$ = 210.3.

*(Z)-Methyl N′-Cyano-N-(p-tolyl)carbamimidothioate (**5c**).* Synthesized according to method A, derivative **5c** was isolated as a white solid (yield 67%); mp 152−154 °C. ^{1}H NMR ($CDCl_3$) δ: 2.38 (s, 3H), 2.43 (s, 3H), 7.14 (dd, J = 9.0 and 2.6 Hz, 2H), 7.19 (dd, J = 9.0 and 2.6 Hz, 2H), 7.97 (bs, 1H). MS (ESI): $[M + 1]^+$ = 206.1.

*(Z)-Methyl N′-Cyano-N-(3-methylphenyl)carbamimidothioate (**5d**).* Synthesized according to method A, derivative **5d** was obtained as a white solid (yield 52%); mp 148−150 °C. ^{1}H NMR ($CDCl_3$) δ: 2.39 (s, 3H), 2.44 (s, 3H), 6.81 (m, 1H), 6.93 (s, 1H), 7.03 (m, 2H), 7.82 (bs, 1H). MS (ESI): $[M + 1]^+$ = 206.2.

*(Z)-Methyl N′-cyano-N-(3,4-dimethylphenyl)-carbamimidothioate (**5e**).* Synthesized according to method A, derivative **5e** was obtained as a white solid (yield 87%); mp 138−140 °C. ^{1}H NMR ($CDCl_3$) δ: 2.27 (s, 6H), 2.43 (s, 3H), 7.05 (m, 2H), 7.14 (d, J = 7.8 Hz, 1H), 7.84 (bs, 1H). MS (ESI): $[M + 1]^+$ = 220.2.

*(Z)-Methyl N′-Cyano-N-(4-ethylphenyl)carbamimidothioate (**5f**).* Synthesized according to method A, compound **5f** was obtained as a white solid (yield 68%); mp 159−161 °C. ^{1}H NMR ($CDCl_3$) δ: 1.25 (t, J = 7.6 Hz, 3H), 2.43 (s, 3H), 2.62 (q, J = 7.6 Hz, 2H), 7.17 (dd, J = 9.0 and 2.8 Hz, 2H), 7.24 (dd, J = 9.0 and 2.8 Hz, 2H), 7.90 (bs, 1H). MS (ESI): $[M + 1]^+$ = 220.4.

*(Z)-Methyl N′-Cyano-N-(4-isopropylphenyl)carbamimidothioate (**5g**).* Synthesized according to method A, derivative **5g** was obtained as a white solid (yield 64%); mp 129−131 °C. ^{1}H NMR ($CDCl_3$) δ: 1.26 (d, J = 7.0 Hz, 6H), 2.44 (s, 3H), 2.93 (m, 1H), 6.89 (dd, J = 8.4 and 2.4 Hz, 2H), 7.22 (dd, J = 8.4 and 2.4 Hz, 2H), 7.93 (bs, 1H). MS (ESI): $[M + 1]^+$ = 234.4.

*(Z)-Methyl N-(4-n-Butylphenyl)-N′-cyanocarbamimidothioate (**5h**).* Synthesized according to method A, derivative **5h** was obtained as a white solid (yield 63%); mp 149−151 °C. ^{1}H NMR ($CDCl_3$) δ: 0.93 (t, J = 7.4 Hz, 3H), 1.33 (m, 2H), 1.59 (m, 2H), 2.43 (s, 3H), 2.63 (t, J = 7.8 Hz, 2H), 7.17 (dd, J = 8.8 and 2.4 Hz, 2H), 7.24 (dd, J = 8.8 and 2.4 Hz, 2H), 7.93 (bs, 1H). MS (ESI): $[M + 1]^+$ = 248.4.

*(Z)-Methyl N′-Cyano-N-(4-methoxyphenyl)carbamimidothioate (**5i**).* Synthesized according to method A, compound **5i** was obtained as a purple solid (yield 91%); mp 193−195 °C. ^{1}H NMR ($CDCl_3$) δ: 2.41 (s, 3H), 3.83 (s, 3H), 6.89 (d, J = 8.8 Hz, 2H), 7.18 (d, J = 8.8 Hz, 2H), 7.97 (bs, 1H). MS (ESI): $[M + 1]^+$ = 222.1.

*(Z)-Methyl N′-Cyano-N-(3-methoxyphenyl)carbamimidothioate (**5j**).* Synthesized according to method A, compound **5j** was obtained as a gray solid (yield 67%); mp 161−163 °C. ^{1}H NMR (DMSO-d_6) δ: 2.69 (s, 3H), 3.75 (s, 3H), 6.82 (ddd, J = 7.4, 2.4, and 1.2 Hz, 1H), 7.00 (m, 2H), 7.03 (m, 1H), 10.1 (bs, 1H). MS (ESI): $[M + 1]^+$ = 222.1.

*(Z)-Methyl N′-Cyano-N-(3,4-dimethoxyphenyl)-carbamimidothioate (**5k**).* Synthesized according to method A, derivative **5k** was obtained as a purple solid (yield 69%); mp 178−180 °C. ^{1}H NMR ($CDCl_3$) δ: 2.42 (s, 3H), 3.89 (s, 3H), 3.90 (s, 3H), 6.86 (m, 3H), 7.95 (bs, 1H). MS (ESI): $[M + 1]^+$ = 252.3.

*(Z)-Methyl N′-Cyano-N-(3,4,5-trimethoxyphenyl)-carbamimidothioate (**5l**).* Synthesized according to method A, compound **5l** was obtained as a gray solid (yield 68%); mp 150−151 °C. ^{1}H NMR ($CDCl_3$) δ: 2.45 (s, 3H), 3.81 (s, 3H), 3.86 (s, 6H), 6.54 (s, 2H), 7.96 (bs, 1H). MS (ESI): $[M + 1]^+$ = 282.3.

*(Z)-Methyl N′-Cyano-N-(4-ethoxyphenyl)carbamimidothioate (**5m**).* Synthesized according to method A, derivative **5m** was obtained as a gray solid (yield 82%); mp 165−167 °C. ^{1}H NMR ($CDCl_3$) δ: 1.43 (t, J = 7.2 Hz, 3H), 2.41 (s, 3H), 4.02 (q, J = 7.2 Hz, 2H), 6.88 (dd, J = 7.0 and 2.2 Hz, 2H), 7.17 (dd, J = 7.0 and 2.2 Hz, 2H), 7.89 (bs, 1H). MS (ESI): $[M + 1]^+$ = 236.2.

*(Z)-Methyl N-Benzo[d][1,3]dioxol-5-yl-N′-cyanocarbamimidothioate (**5n**).* Synthesized according to method A, derivative **5n** was obtained as a white solid (yield 73%); mp 191−193 °C. ^{1}H NMR ($CDCl_3$) δ: 2.42 (s, 3H), 6.04 (s, 2H), 6.79 (m, 3H), 7.81 (bs, 1H). MS (ESI): $[M + 1]^+$ = 236.2.

General Procedure B for the Synthesis of Compounds 6a−n. To a stirred suspension of derivative **5a−n** (2 mmol) in dry THF (10 mL) was added hydrazine monohydrate (0.1 mL, 2 mmol, 1 equiv), and the reaction mixture was heated under reflux for 6 h. After this time, the suspension was evaporated in vacuo to dryness, and the residue was suspended with ethyl ether (10 mL) and stirred for 10 min. The resultant solid was collected by filtration and then used for the next reaction without any purification.

*N^3-Phenyl-1H-1,2,4-triazole-3,5-diamine (**6a**).* Synthesized according to general procedure B, derivative **6a** was obtained as a white solid (yield 74%); mp 160−161 °C. ^{1}H NMR (DMSO-d_6) δ: 5.83 (bs, 2H), 6.71 (t, J = 7.8 Hz, 1H), 7.14 (t, J = 7.8 Hz, 2H), 7.46 (d, J = 8.4 Hz, 2H), 8.57 (bs, 1H), 11.1 (bs, 1H). MS (ESI): $[M + 1]^+$ = 176.1.

*N^3-(4-Fluorophenyl)-1H-1,2,4-triazole-3,5-diamine (**6b**).* Synthesized according to general procedure B, derivative **6b** was obtained as a white solid (yield 83%); mp 216−218 °C. ^{1}H NMR (DMSO-d_6) δ: 5.84 (bs, 2H), 6.98 (t, J = 8.8 Hz, 2H), 7.48 (m, 2H), 8.61 (bs, 1H), 11.1 (bs, 1H). MS (ESI): $[M + 1]^+$ = 194.2.

*N^3-(p-Tolyl)-1H-1,2,4-triazole-3,5-diamine (**6c**).* Synthesized according to general procedure B, compound **6c** was obtained as a white solid (yield 92%); mp 185−187 °C. ^{1}H NMR (DMSO-d_6) δ: 2.19 (s, 3H), 5.81 (bs, 2H), 6.93 (d, J = 8.6 Hz, 2H), 7.36 (dd, J = 8.6 Hz, 2H), 8.42 (bs, 1H), 11.0 (bs, 1H). MS (ESI): $[M + 1]^+$ = 190.2.

*N^3-(m-Tolyl)-1H-1,2,4-triazole-3,5-diamine (**6d**).* Synthesized according to general procedure B, compound **6d** was obtained as a white solid (yield >95%); mp 112−114 °C. ^{1}H NMR (DMSO-d_6) δ: 2.21 (s, 3H), 5.81 (bs, 2H), 6.51 (d, J = 7.2 Hz, 1H), 7.02 (t, J = 7.2 Hz, 1H), 7.24 (d, J = 7.2 Hz, 1H), 7.33 (s, 1H), 8.49 (bs, 1H), 11.1 (bs, 1H). MS (ESI): $[M + 1]^+$ = 220.2.

*N^3-(3,4-Dimethylphenyl)-1H-1,2,4-triazole-3,5-diamine (**6e**).* Synthesized according to general procedure B, derivative **6e** was obtained as a white solid (yield >95%); mp 180−182 °C. ^{1}H NMR (DMSO-d_6) δ: 2.10 (s, 3H), 2.13 (s, 3H), 5.77 (bs, 2H), 6.86 (d, J = 8.2 Hz, 1H), 7.18 (d, J = 8.2 Hz, 1H), 7.26 (s, 1H), 8.35 (bs, 1H), 11.0 (bs, 1H). MS (ESI): $[M + 1]^+$ = 204.3.

*N^3-(4-Ethylphenyl)-1H-1,2,4-triazole-3,5-diamine (**6f**).* Synthesized according to general procedure B, compound **6f** was obtained as a white solid (yield 92%); mp 187−189 °C. ^{1}H NMR (DMSO-d_6) δ: 1.13 (t, J = 7.6 Hz, 3H), 2.47 (q, J = 7.6 Hz, 2H), 5.80 (bs, 2H), 6.96 (d, J = 8.4 Hz, 2H), 7.37 (d, J = 8.4 Hz, 2H), 8.42 (bs, 1H), 11.0 (bs, 1H). MS (ESI): $[M + 1]^+$ = 204.3.

*N^3-(4-Isopropylphenyl)-1H-1,2,4-triazole-3,5-diamine (**6g**).* Synthesized according to general procedure B, compound **6g** was obtained as a white solid (yield 60%); mp 156−158 °C. ^{1}H NMR (DMSO-d_6) δ: 1.17 (d, J = 6.8 Hz, 6H), 2.76 (m, 1H), 5.77 (bs, 2H), 6.99 (d, J = 8.6 Hz, 2H), 7.37 (d, J = 8.6 Hz, 2H), 8.44 (bs, 1H), 11.0 (bs, 1H). MS (ESI): $[M + 1]^+$ = 218.2.

*N^3-(4-n-Butylphenyl)-1H-1,2,4-triazole-3,5-diamine (**6h**).* Synthesized according to general procedure B, derivative **6h** was obtained as a white solid (yield 66%); mp 177−179 °C. ^{1}H NMR (DMSO-d_6) δ: 0.88 (t, J = 7.0 Hz, 3H), 1.26 (m, 2H), 1.48 (m, 2H), 2.41 (t, J = 7.6 Hz, 2H), 5.80 (bs, 2H), 6.94 (d, J = 8.2 Hz, 2H), 7.36 (dd, J = 8.2 Hz, 2H), 8.43 (bs, 1H), 11.1 (bs, 1H). MS (ESI): $[M + 1]^+$ = 232.3.

*N^3-(4-Methoxyphenyl)-1H-1,2,4-triazole-3,5-diamine (**6i**).* Synthesized according to general procedure B, derivative **6i** was obtained as a gray solid (yield 88%); mp 200−201 °C. ^{1}H NMR (DMSO-d_6) δ: 3.67 (s, 3H), 5.76 (bs, 2H), 6.74 (dd, J = 7.0 and 2.2 Hz, 2H), 7.39 (dd, J = 7.0 and 2.2 Hz, 2H), 8.32 (bs, 1H), 11.0 (bs, 1H). MS (ESI): $[M + 1]^+$ = 206.3.

*N^3-(3-Methoxyphenyl)-1H-1,2,4-triazole-3,5-diamine (**6j**).* Synthesized according to general procedure B, derivative **6j** was obtained as a red solid (yield >95%); mp 117−119 °C. ^{1}H NMR (DMSO-d_6) δ: 3.76 (s, 3H), 5.78 (bs, 2H), 6.88 (dd, J = 7.4 and 2.4 Hz, 1H), 7.02 (m, 2H), 7.05 (m, 1H), 8.47 (bs, 1H), 11.1 (bs, 1H). MS (ESI): $[M + 1]^+$ = 206.2.

*N^3-(3,4-Dimethoxyphenyl)-1H-1,2,4-triazole-3,5-diamine (**6k**).* Synthesized according to general procedure B, derivative **6k** was obtained as a purple solid (yield 72%); mp 158−160 °C. ^{1}H NMR (DMSO-d_6) δ: 3.66 (s, 3H), 3.75 (s, 3H), 5.75 (bs, 2H), 6.74 (d, J =

dx.doi.org/10.1021/jm5008193 | J. Med. Chem. XXXX, XXX, XXX−XXX

8.8 Hz, 1H), 6.98 (m, 1H), 7.23 (d, J = 2.4 Hz, 1H), 8.32 (bs, 1H), 11.2 (bs, 1H). MS (ESI): $[M + 1]^+$ = 236.2.

*N^3-(3,4,5-Trimethoxyphenyl)-1H-1,2,4-triazole-3,5-diamine (**6l**).* Synthesized according to general procedure B, derivative **6l** was obtained as a white solid (yield 68%); mp 241−243 °C. ^{1}H NMR (DMSO-d_6) δ: 3.56 (s, 3H), 3.70 (s, 6H), 5.84 (bs, 2H), 6.90 (s, 2H), 8.43 (bs, 1H), 11.1 (bs, 1H). MS (ESI): $[M + 1]^+$ = 266.3.

*N^3-(4-Ethoxyphenyl)-1H-1,2,4-triazole-3,5-diamine (**6m**).* Synthesized according to general procedure B, derivative **6m** was obtained as a purple solid (yield 94%); mp 200−201 °C. ^{1}H NMR (DMSO-d_6) δ: 1.28 (t, J = 7.0 Hz, 3H), 3.93 (q, J = 7.0 Hz, 2H), 5.76 (bs, 2H), 6.72 (dd, J = 7.0 and 2.0 Hz, 2H), 7.38 (dd, J = 7.0 and 2.0 Hz, 2H), 8.31 (bs, 1H), 11.0 (bs, 1H). MS (ESI): $[M + 1]^+$ = 220.2.

*N^3-(Benzo[d][1,3]dioxol-5-yl)-1H-1,2,4-triazole-3,5-diamine (**6n**).* Synthesized according to general procedure B, compound **6n** was obtained as a brown solid (yield 73%); mp 206−208 °C. ^{1}H NMR (DMSO-d_6) δ: 5.80 (bs, 2H), 5.88 (s, 2H), 6.69 (d, J = 8.2 Hz, 1H), 6.87 (dd, J = 8.2 and 2.2 Hz, 1H), 7.26 (d, J = 2.2 Hz, 1H), 8.45 (bs, 1H), 11.1 (bs, 1H). MS (ESI): $[M + 1]^+$ = 220.2.

General Procedure C for the Synthesis of Compounds 3a−n and 7a−n. To a stirred solution of the appropriate 1,2,4-triazole **6a−n** (1 mmol) in dry pyridine (10 mL) cooled at −5 °C was added 3′,4′,5′-trimethoxybenzoyl chloride (230 mg, 1.1 mol, 1.1 equiv) in small portions. The reaction mixture was kept for 30 min at −5 °C and then overnight at room temperature. Pyridine was then removed by evaporation under reduced pressure. To the residue was added CH_2Cl_2, and the organic phase was washed with saturated aq $NaHCO_3$, water, and brine and dried over Na_2SO_4. The reaction mixture was filtered, and the solvent was removed in vacuo. The crude residue was purified by column chromatography on silica gel using a mixture of CH_2Cl_2−methanol (9.5:0.5) as eluent to separate the two regioisomeric 3′,4′,5′-trimethoxybenzoyl triazoles **3a−n** and **7a−n**, with the former compounds **3a−n** characterized by the lower R_f.

*(3-(Phenylamino)-5-amino-1H-1,2,4-triazol-1-yl)(3,4,5-trimethoxyphenyl) Methanone (**3a**).* Synthesized according to method C, derivative **3a** was obtained as a yellow solid (yield 56%); mp 181−183 °C. ^{1}H NMR (DMSO-d_6) δ: 3.79 (s, 3H), 3.86 (s, 6H), 6.86 (t, J = 7.2 Hz, 1H), 7.22 (t, J = 8.4 Hz, 2H), 7.56 (d, J = 7.6 Hz, 2H), 7.68 (s, 2H), 7.93 (bs, 2H), 9.35 (s, 1H). ^{13}C NMR (DMSO-d_6) δ: 55.96 (2C), 60.23, 108.66 (2C), 116.57 (2C), 120.37, 127.17, 128.57 (2C), 140.89, 141.37, 152.07 (2C), 157.58, 158.19, 165.37. MS (ESI): $[M]^+$ = 369.8. Anal. ($C_{18}H_{19}N_5O_4$) C, H, N.

*(3-(4-Fluorophenylamino)-5-amino-1H-1,2,4-triazol-1-yl)(3,4,5-trimethoxyphenyl) Methanone (**3b**).* Synthesized according to method C, compound **3b** was obtained as a yellow solid (yield 60%); mp 218−220 °C. ^{1}H NMR (DMSO-d_6) δ: 3.79 (s, 3H), 3.86 (s, 6H), 7.07 (t, J = 8.8 Hz, 2H), 7.56 (dd, J = 8.8 and 3.4 Hz, 2H), 7.61 (s, 2H), 7.83 (bs, 2H), 9.38 (s, 1H). ^{13}C NMR (DMSO-d_6) δ: 55.98 (2C), 60.22, 108.58 (2C), 114.99, 115.21, 117.81, 117.88, 127.15, 137.40, 141.35, 152.08 (2C), 155.17, 157.60, 158.19, 165.41. MS (ESI): $[M]^+$ = 387.7. Anal. ($C_{18}H_{18}FN_5O_4$) C, H, N.

*(3-(4-Tolylamino)-5-amino-1H-1,2,4-triazol-1-yl)(3,4,5-trimethoxyphenyl) Methanone (**3c**).* Synthesized according to method C, compound **3c** was obtained as a yellow solid (yield 55%); mp 235−237 °C. ^{1}H NMR (DMSO-d_6) δ: 2.22 (s, 3H), 3.79 (s, 3H), 3.88 (s, 6H), 6.97 (d, J = 8.6 Hz, 2H), 7.44 (d, J = 8.6 Hz, 2H), 7.68 (s, 2H), 7.81 (bs, 2H), 9.22 (s, 1H). ^{13}C NMR (DMSO-d_6) δ: 20.26, 95.96 (2C), 60.22, 108.63 (2C), 116.68 (2C), 120.36, 127.20, 128.87 (2C), 138.41, 141.32, 152.15 (2C), 157.56, 158.26, 165.33. MS (ESI): $[M]^+$ = 383.5. Anal. ($C_{19}H_{21}N_5O_4$) C, H, N.

*(3-(3-Tolylamino)-5-amino-1H-1,2,4-triazol-1-yl)(3,4,5-trimethoxyphenyl) Methanone (**3d**).* Synthesized according to method C, derivative **3d** was obtained as a yellow solid (yield 61%); mp 165−167 °C. ^{1}H NMR (DMSO-d_6) δ: 2.30 (s, 3H), 3.78 (s, 3H), 3.85 (s, 6H), 6.65 (d, J = 7.4 Hz, 1H), 7.08 (t, J = 7.8 Hz, 1H), 7.34 (s, 1H), 7.39 (d, J = 7.8 Hz, 1H), 7.61 (s, 2H), 7.80 (bs, 2H), 9.26 (s, 1H). ^{13}C NMR (DMSO-d_6) δ: 21.26, 55.99 (2C), 60.22, 108.52 (2C), 113.77, 117.16, 120.98, 127.40, 128.38, 137.70, 140.87, 141.20, 152.05 (2C), 157.40, 158.14, 165.63. MS (ESI): $[M]^+$ = 383.5. Anal. ($C_{19}H_{21}N_5O_4$) C, H, N.

*(3-(3,4-Dimethylphenylamino)-5-amino-1H-1,2,4-triazol-1-yl)-(3,4,5-trimethoxyphenyl) Methanone (**3e**).* Synthesized according to method C, compound **3e** was obtained as a yellow solid (yield 48%); mp 169−171 °C. ^{1}H NMR (DMSO-d_6) δ: 2.12 (s, 6H), 3.80 (s, 3H), 3.85 (s, 6H), 6.93 (d, J = 8.0 Hz, 1H), 7.31 (s, 1H), 7.35 (d, J = 8.0 Hz, 1H), 7.61 (s, 2H), 7.78 (bs, 2H), 9.14 (s, 1H). ^{13}C NMR (DMSO-d_6) δ: 18.61, 19.75, 55.98 (2C), 60.22, 108.51 (2C), 114.01, 117.93, 127.45, 127.69, 129.42, 136.11, 138.74, 141.17, 152.03 (2C), 157.38, 158.21, 165.57. MS (ESI): $[M]^+$ = 397.7. Anal. ($C_{20}H_{23}N_5O_4$) C, H, N.

*(3-(4-Ethylphenylamino)-5-amino-1H-1,2,4-triazol-1-yl)(3,4,5-trimethoxyphenyl) Methanone (**3f**).* Synthesized according to method C, compound **3f** was obtained as a yellow solid (yield 54%); mp 194−196 °C. ^{1}H NMR (DMSO-d_6) δ: 1.14 (t, J = 8.4 Hz, 3H), 3.51 (d, J = 8.4 Hz, 2H), 3.78 (s, 3H), 3.97 (s, 6H). 7.02 (d, J = 8.6 Hz, 2H), 7.46 (d, J = 8.6 Hz, 2H), 7.68 (s, 2H), 7.81 (bs, 2H), 8.22 (s, 1H). ^{13}C NMR (DMSO-d_6) δ: 16.35, 31.15, 56.41 (2C), 61.68, 109.07 (2C), 127.14 (2C), 127.66, 128.22 (2C), 135.97, 139.08, 141.76, 152.50 (2C), 156.03, 158.74, 165.78. MS (ESI): $[M]^+$ = 397.5. Anal. ($C_{21}H_{26}N_5O_4$) C, H, N.

*(3-(4-Isopropylphenylamino)-5-amino-1H-1,2,4-triazol-1-yl)-(3,4,5-trimethoxyphenyl) Methanone (**3g**).* Synthesized according to method C, derivative **3g** was obtained as a yellow solid (yield 52%); mp 197−199 °C. ^{1}H NMR (DMSO-d_6) δ: 1.14 (d, J = 6.8 Hz, 6H), 2.80 (m, 1H), 3.77 (s, 3H), 3.87 (s, 6H), 7.06 (d, J = 8.2 Hz, 2H), 7.46 (d, J = 8.2 Hz, 2H), 7.68 (s, 2H), 7.81 (bs, 2H), 9.21 (s, 1H). ^{13}C NMR (DMSO-d_6) δ: 24.06 (2C), 32.65, 55.95 (2C), 60.23, 108.65 (2C), 116.75 (2C), 120.39 (2C), 124.28, 126.24, 138.70, 140.25, 152.05 (2C), 157.58, 158.32, 165.32. MS (ESI): $[M]^+$ = 411.7. Anal. ($C_{21}H_{25}N_5O_4$) C, H, N.

*(3-(4-Butylphenylamino)-5-amino-1H-1,2,4-triazol-1-yl)(3,4,5-trimethoxyphenyl) Methanone (**3h**).* Synthesized according to method C, compound **3h** was obtained as a yellow solid (yield 54%); mp 134−136 °C. ^{1}H NMR (DMSO-d_6) δ: 0.88 (t, J = 7.2 Hz, 3H), 1.29 (m, 2H), 1.50 (m, 2H), 2.44 (t, J = 7.6 Hz, 2H), 3.80 (s, 3H), 3.87 (s, 6H), 7.00 (d, J = 8.6 Hz, 2H), 7.45 (d, J = 8.6 Hz, 2H), 7.68 (s, 2H), 7.81 (bs, 2H), 9.22 (s, 1H). ^{13}C NMR (DMSO-d_6) δ: 13.78, 21.66, 33.36, 34.09, 55.94 (2C), 60.23, 108.64 (2C), 116.67 (2C), 120.38, 127.21, 128.30 (2C), 134.05, 138.61, 152.05 (2C), 157.57, 158.29, 165.33. MS (ESI): $[M]^+$ = 425.8. Anal. ($C_{22}H_{27}N_5O_4$) C, H, N.

*(3-(4-Methoxyphenylamino)-5-amino-1H-1,2,4-triazol-1-yl)-(3,4,5-trimethoxyphenyl) Methanone (**3i**).* Synthesized according to method C, compound **3i** was obtained as a yellow solid (yield 64%); mp 196−197 °C. ^{1}H NMR (DMSO-d_6) δ: 3.67 (s, 3H), 3.77 (s, 3H), 3.84 (s, 6H), 6.77 (d, J = 8.8 Hz, 2H), 7.46 (d, J = 8.8 Hz, 2H), 7.66 (s, 2H), 7.79 (bs, 2H), 9.11 (s, 1H). ^{13}C NMR (DMSO-d_6) δ: 55.07, 55.85 (2C), 60.13, 108.53 (2C), 113.76 (2C), 127.81 (2C), 127.11, 134.24, 141.21, 151.95 (2C), 153.19, 157.48, 158.29, 165.16. MS (ESI): $[M]^+$ = 399.8. Anal. ($C_{19}H_{21}N_5O_5$) C, H, N.

*(3-(3-Methoxyphenylamino)-5-amino-1H-1,2,4-triazol-1-yl)-(3,4,5-trimethoxyphenyl) Methanone (**3j**).* Synthesized according to method C, compound **3j** was obtained as a yellow solid (yield 42%); mp 178−180 °C. ^{1}H NMR (DMSO-d_6) δ: 3.65 (s, 3H), 3.78 (s, 3H), 3.86 (s, 6H), 6.44 (m, 1H), 7.12 (m, 2H), 7.26 (s, 1H), 7.61 (s, 2H), 7.81 (bs, 2H), 9.32 (s, 1H). ^{13}C NMR (DMSO-d_6) δ: 54.76, 55.94 (2C), 60.19, 102.99, 105.19, 108.45 (2C), 109.37, 127.36, 129.29, 141.22, 142.01, 152.07 (2C), 157.45, 158.12, 159.78, 165.63. MS (ESI): $[M]^+$ = 399.6. Anal. ($C_{19}H_{21}N_5O_5$) C, H, N.

*(3-(3,4-Dimethoxyphenylamino)-5-amino-1H-1,2,4-triazol-1-yl)-(3,4,5-trimethoxyphenyl) Methanone (**3k**).* Synthesized according to method C, derivative **3k** was obtained as a yellow solid (yield 51%); mp 170−171 °C. ^{1}H NMR (DMSO-d_6) δ: 3.67 (s, 3H), 3.73 (s, 3H), 3.77 (s, 3H), 3.83 (s, 6H), 6.77 (d, J = 8.6 Hz, 1H), 7.08 (dd, J = 8.6 and 2.2 Hz, 1H), 7.22 (d, J = 2.2 Hz, 1H), 7.56 (s, 2H), 7.78 (bs, 2H), 9.09 (s, 1H). ^{13}C NMR (DMSO-d_6) δ: 55.16 (2C), 56.00 (2C), 60.20, 102.58, 108.25, 108.33 (2C), 112.61, 127.61, 134.95, 141.06, 142.85, 148.90, 152.02 (2C), 157.35, 158.28, 165.71. MS (ESI): $[M]^+$ = 429.8. Anal. ($C_{20}H_{23}N_5O_6$) C, H, N.

*(3-(3,4,5-Trimethoxyphenylamino)-5-amino-1H-1,2,4-triazol-1-yl)(3,4,5-trimethoxyphenyl) Methanone (**3l**).* Synthesized according to method C, derivative **3l** was obtained as a yellow solid (yield 48%);

dx.doi.org/10.1021/jm5008193 | J. Med. Chem. XXXX, XXX, XXX−XXX

mp 172−174 °C. ^{1}H NMR (DMSO-d_6) δ: 3.56 (s, 3H), 3.58 (s, 3H), 3.75 (s, 6H), 3.79 (s, 6H), 6.91 (s, 2H), 7.41 (s, 2H), 7.75 (bs, 2H), 9.16 (s, 1H). ^{13}C NMR (DMSO-d_6) δ: 55.44 (2C), 56.08 (2C), 60.17 (2C), 94.92 (2C), 108.04 (2C), 128.01, 131.38, 137.16, 140.87, 151.98 (2C), 152.84 (2C), 157.09, 158.09, 166.29. MS (ESI): $[M]^+$ = 459.8. Anal. ($C_{21}H_{25}N_5O_7$) C, H, N.

*(3-(4-Ethoxyphenylamino)-5-amino-1H-1,2,4-triazol-1-yl)(3,4,5-trimethoxyphenyl) Methanone (**3m**).* Synthesized according to method C, compound **3c** was obtained as a yellow solid (yield 54%); mp 176−178 °C. ^{1}H NMR (DMSO-d_6) δ: 1.29 (t, J = 6.8 Hz, 3H), 3.79 (s, 3H), 3.86 (s, 6H), 3.93 (q, J = 6.8 Hz, 2H), 6.77 (d, J = 9.0 H, 2H), 7.46 (d, J = 9.0 H, 2H), 7.68 (s, 2H), 7.80 (bs, 2H), 9.11 (s, 1H). ^{13}C NMR (DMSO-d_6) δ: 14.73, 55.95 (2C), 60.22, 63.09, 108.62 (2C), 114.44 (2C), 127.86 (2C), 127.22, 134.27, 141.29, 152.05 (2C), 152.51, 157.57, 158.38, 165.25. MS (ESI): $[M]^+$ = 413.8. Anal. ($C_{20}H_{23}N_5O_5$) C, H, N.

*(5-Amino-3-(benzo[d][1,3]dioxol-5-ylamino)-1H-1,2,4-triazol-1-yl)(3,4,5-trimethoxyphenyl) Methanone (**3n**).* Synthesized according to method C, compound **3n** was obtained as a yellow solid (yield 46%); mp 200−201 °C. ^{1}H NMR (DMSO-d_6) δ: 3.78 (s, 3H), 3.86 (s, 6H), 5.93 (s, 2H), 6.76 (d, J = 8.4 Hz, 1H), 6.92 (dd, J = 8.4 and 2.2 Hz, 1H), 7.33 (d, J = 2.2 Hz, 1H), 7.65 (s, 2H), 7.81 (bs, 2H), 9.23 (s, 1H). ^{13}C NMR (DMSO-d_6) δ: 55.97 (2C), 60.22, 99.01, 100.67, 108.12, 108.51 (2C), 108.93, 127.25, 135.73, 140.71, 141.28, 147.23, 152.06 (2C), 157.53, 158.26, 165.34. MS (ESI): $[M]^+$ = 413.8. Anal. ($C_{19}H_{19}N_5O_6$) C, H, N.

X-ray Structure Determination. X-ray diffraction data for compound **3c** were collected at room temperature, 295 K, on a Nonius Kappa CCD diffractometer with graphite monochromated Mo Kα radiation (λ = 0.7107 Å). The structure was solved by direct methods (SIR97)[35] and refined (SHELXL-97)[36] by full matrix least-squares with anisotropic non-hydrogen atoms. The hydrogen atoms were included on calculated positions, riding on their carrier atoms, except for those bound to nitrogen. The latter were refined isotropically.

Crystal Data. $C_{19}H_{21}N_5O_4$; orthorhombic, space group *Pbca*, a = 7.6945(1), b = 18.7364(4), c = 26.0711(5) Å, V = 3758.6(1) Å^3, Z = 8, D_c = 1.355 g cm^{-3}. Intensity data collected with $\theta \leq 26°$; 3677 independent reflections measured; 2412 observed [$I > 2\sigma(I)$]. Final R index = 0.0471 (observed reflections), R_w = 0.1395 (all reflections), S = 1.022. Complete crystallographic data have been deposited with the Cambridge Crystallographic Data Centre as supplementary publication number CCDC no. 984800. Copies of that data can be obtained, free of charge, via www.ccdc.cam.ac.uk./conts/retrieving.html or on application to CCDC, 12 Union Road, Cambridge CB2 1EZ, U.K. [fax: +44(0)-1223-336033, e-mail: deposit@ccdc.cam.ac.uk].

Cell Growth Conditions and Antiproliferative Assay. Human T-leukemia (CCRF-CEM and Jurkat) and human B-leukemia (SEM) cells were grown in RPMI-1640 medium (Gibco, Milano, Italy). Breast adenocarcinoma (MCF-7), human cervix carcinoma (HeLa), and human colon adenocarcinoma (HT-29) cells were grown in DMEM medium (Gibco, Milano, Italy), all supplemented with 115 units/mL penicillin G (Gibco, Milano, Italy), 115 μg/mL streptomycin (Invitrogen, Milano, Italy), and 10% fetal bovine serum (Invitrogen, Milano, Italy). CEM$^{Vbl\text{-}100}$ cells are a multidrug-resistant line selected against vinblastine.[20] LoVo^{Doxo} cells are a doxorubicin resistant subclone of LoVo cells[21] and were grown in complete Ham's F12 medium supplemented with doxorubicin (0.1 μg/mL). LoVo^{Doxo} and CEM$^{Vbl\text{-}100}$ were a kind gift of Dr. G. Arancia (Istituto Superiore di Sanità, Rome, Italy). Stock solutions (10 mM) of the different compounds were obtained by dissolving them in DMSO. Individual wells of a 96-well tissue culture microtiter plate were inoculated with 100 μL of complete medium containing 8 × 10^3 cells. The plates were incubated at 37 °C in a humidified 5% CO_2 incubator for 18 h prior to the experiments. After medium removal, 100 μL of fresh medium containing the test compound at different concentrations was added to each well in triplicate and incubated at 37 °C for 72 h. The percentage of DMSO in the medium never exceeded 0.25%. This was also the maximum DMSO concentration in all cell-based assays described below. Cell viability was assayed by the (3-(4,5-dimethylthiazol-2-yl)-2,5-diphenyltetrazolium bromide test as previously described.[37] The IC_{50} was defined as the compound concentration required to inhibit cell proliferation by 50% in comparison with cells treated with the maximum amount of DMSO (0.25%) and considered as 100% viability.

Peripheral blood lymphocytes (PBL) from healthy donors were obtained by separation on Lymphoprep (Fresenius KABI Norge AS) gradient. After extensive washing, cells were resuspended (1.0 × 10^6 cells/mL) in RPMI-1640 with 10% fetal bovine serum and incubated overnight. For cytotoxicity evaluations in proliferating PBL cultures, nonadherent cells were resuspended at 5 × 10^5 cells/mL in growth medium, containing 2.5 μg/mL PHA (Irvine Scientific). Different concentrations of the test compounds were added, and viability was determined 72 h later by the MTT test. For cytotoxicity evaluations in resting PBL cultures, nonadherent cells were resuspended (5 × 10^5 cells/mL) and treated for 72 h with the test compounds, as described above.

Effects on Tubulin Polymerization and on Colchicine Binding to Tubulin. To evaluate the effect of the compounds on tubulin assembly in vitro,[38a] varying concentrations of compounds were preincubated with 10 μM bovine brain tubulin in 0.8 M monosodium glutamate (pH adjusted to 6.6 with HCl in a 2.0 M stock solution) at 30 °C and then cooled to 0 °C. After addition of 0.4 mM GTP, the mixtures were transferred to 0 °C cuvettes in a recording spectrophotometer and warmed to 30 °C. Tubulin assembly was followed turbidimetrically at 350 nm. The IC_{50} was defined as the compound concentration that inhibited the extent of assembly by 50% after a 20 min incubation. The capacity of the test compounds to inhibit colchicine binding to tubulin was measured as described,[38b] except that the reaction mixtures contained 1 μM tubulin, 5 μM [^{3}H]colchicine, and 5 μM test compound.

Molecular Modeling. All molecular modeling studies were performed on a MacPro dual 2.66 GHz Xeon running Ubuntu 12.04. The tubulin structure was downloaded from the PDB data bank (http://www.rcsb.org/; PDB code 1SA0).[39] Hydrogen atoms were added to the protein, using the Protonate 3D routine of the Molecular Operating Environment (MOE).[40] Ligand structures were built with MOE and minimized using the MMFF94x force field until a RMSD gradient of 0.05 kcal mol^{-1} Å^{-1} was reached. The docking simulations were performed using PLANTS.[41]

Flow Cytometric Analysis of Cell Cycle Distribution. HeLa or Jurkat cells (5 ×10^5) were treated with different concentrations of the test compounds for 24 h. After the incubation period, the cells were collected, centrifuged, and fixed with ice-cold ethanol (70%). The cells were then treated with lysis buffer containing RNase A and 0.1% Triton X-100 and then stained with PI. Samples were analyzed on a Cytomic FC500 flow cytometer (Beckman Coulter). DNA histograms were analyzed using MultiCycle for Windows (Phoenix Flow Systems).

Apoptosis Assay. Cell death was determined by flow cytometry of cells double stained with annexin V/FITC and PI. The Coulter Cytomics FC500 (Beckman Coulter) was used to measure the surface exposure of PS on apoptotic cells according to the manufacturer's instructions (Annexin-V Fluos, Roche Diagnostics).

Western Blot Analysis. HeLa cells were incubated in the presence of **3c** and after different times were collected, centrifuged, and washed two times with ice-cold phosphate buffered saline (PBS). The pellet was then resuspended in lysis buffer. After the cells were lysed on ice for 30 min, lysates were centrifuged at 15000g at 4 °C for 10 min. The protein concentration in the supernatant was determined using the BCA protein assay reagents (Pierce, Italy). Equal amounts of protein (10 μg) were resolved using sodium dodecyl sulfate-polyacrylamide gel electrophoresis (SDS-PAGE) (7.5−15% acrylamide gels) and transferred to PVDF Hybond-P membrane (GE Healthcare). Membranes were blocked with a bovine serum albumin (BSA) solution (BSA 5% in Tween PBS 1×), the membranes being gently rotated overnight at 4 °C. Membranes were then incubated with primary antibodies against Bcl-2, Bax, PARP, cleaved caspase-9, cdc25c (Cell Signaling), caspase-3 (Alexis), H2AX (Cell Signaling), p53 (Cell Signaling), cyclin B (Cell Signaling), p-cdc2^{Tyr15} (Cell Signaling), p21 (Cell Signaling), or β-

dx.doi.org/10.1021/jm5008193 | J. Med. Chem. XXXX, XXX, XXX−XXX

actin (Sigma-Aldrich) for 2 h at room temperature. Membranes were next incubated with peroxidase-labeled secondary antibodies for 60 min. All membranes were visualized using ECL Select (GE Healthcare) and exposed to Hyperfilm MP (GE Healthcare). To ensure equal protein loading, each membrane was stripped and reprobed with anti-β-actin antibody.

Antivascular Activity. HUVECs were prepared from human umbilical cord veins, as previously described.[33] The adherent cells were maintained in M200 medium supplemented with low serum growth supplement (LSGS), containing FBS, hydrocortisone, hEGF, bFGF, heparin, and gentamycin/amphotericin (Life Technologies, Monza, Italy). Once confluent, the cells were detached by trypsin−EDTA solution and used in experiments from the first to sixth passages.

The motility assay for HUVECs was based on "scratch" wounding of a confluent monolayer.[42] Briefly, HUVECs (1×10^5) were seeded onto 0.1% collagen type I (BD Biosciences, Italy)-coated six-well plates in complete medium until a confluent monolayer was formed. The cells were wounded using a pipet tip, and wells were washed with PBS to remove the detached cells. Then the cells were treated with the test compounds, and at different times from the scratch, the cells were photographed under a light microscope. At all indicated time points, the wound width was measured in four areas and compared with the initial width.

Matrigel matrix (Basement Membrane Matrix, BD Biosciences, Italy) was kept at 4 °C for 3 h, when 230 μL of Matrigel solution was added to each well of a 24-well plate. After gelling at 37 °C for 30 min, gels were overlaid with 500 μL of medium containing 6×10^4 HUVECs. The cells were incubated over Matrigel for 6 h to allow capillary tubes to form. Different concentrations of test compound were added in the cultures and incubated for different times, and the disappearance of existing vasculature was monitored and photographed (five fields for each well: the four quadrants and the center) at a 10× magnification. Phase contrast images were recorded using a digital camera and saved as TIFF files. Image analysis was carried out using the ImageJ image analysis software, and the following dimensional parameters (percent area covered by HUVECs and total length of HUVECs network per field) and topological parameters (number of meshes and branching points per fields) were estimated.[32] Values were expressed as percent change from control cultures grown with complete medium.

Antitumor Activity in Vivo. The in vivo cytotoxic activity of compound **3c** was investigated using a syngeneic murine hepatocellular carcinoma cell line (BNL 1ME A.7R.1) in Balb/c mice.[34] Male mice, 8 weeks old, were purchased from Harlan (S. Pietro al Natisone Udine, Italy), and tumors were induced by a subcutaneous injection in their dorsal region of 10^7 cells in 200 μL of sterile PBS. Animals were randomly divided into four groups, and, starting on the second day, the first group was daily dosed intraperitoneally (ip) with 7 μL/kg of free vehicle (0.9% NaCl containing 5% polyethylene glycol 400 and 0.5% Tween 80). Groups two and three were treated with compound **3c** at the doses of 5 and 10 mg/kg body weight, respectively. The fourth group received the reference compound CA-4P at the dose of 5 mg/kg body weight. Both compound **3c** and CA-4P were dissolved in free vehicle. Tumor sizes were measured daily for 7 days using a pair of calipers. In particular, the tumor volume (V) was calculated by the rotational ellipsoid formula: $V = A \times B2/2$, where A is the longer diameter (axial) and B is the shorter diameter (rotational). All experimental procedures followed guidelines recommended by the Institutional Animal Care and Use Committee of Padova University.

Statistical Analysis. Unless indicated otherwise, the results are presented as the mean ± SEM. The differences between different treatments were analyzed using the two-sided Student's t test. P values lower than 0.05 were considered significant.

■ ASSOCIATED CONTENT

Ⓢ Supporting Information

Detailed characterization of synthesized compounds **7a−c**, **7g−h**, and **7k−l**. Immunofluorescence analysis of tubulin network and apoptosis assay on HeLa cells. This material is available free of charge via the Internet at http://pubs.acs.org.

■ AUTHOR INFORMATION

Corresponding Authors

*For R.R.: phone, 39-(0)532-455303; fax, 39-(0)532-455953; E-mail, rmr@unife.it.

*For P.G.B.: phone, 39-(0)532-455293; fax, 39-(0)532-455953; E-mail, pgb@unife.it.

*For G.V.: phone, 39-(0)49-8211451; fax, 39-(0)49-8211462; E-mail, giampietro.viola1@unipd.it.

Notes

The authors declare no competing financial interest.

■ ACKNOWLEDGMENTS

We thank Alberto Casolari for technical assistance.

■ ABBREVIATIONS USED

CA-4, combretastatin A-4; VDA, vascular disrupting agent; PI, propidium iodide; PS, phosphatidylserine; PARP, polyADP-ribose polymerase; PBL, peripheral blood lymphocytes; PHA, phytohemaglutinin; FITC, fluorescein isothiocyanate; BSA, bovine serum albumin; HE, hydroxyethidine; PBS, phosphate-buffered saline; SDS-PAGE, sodium dodecyl sulfate polyacrylamide gel electrophoresis; HUVEC, human umbilical vein endothelial cell; LSGS, low serum growth supplement

■ REFERENCES

(1) (a) Amos, L. A. What tubulin drugs tell us about microtubule structure and dynamics. *Semin. Cell Dev. Biol.* **2011**, *22*, 916−926. (b) Amos, L. A. Microtubule structure and its stabilisation. *Org. Biomol. Chem.* **2004**, *2*, 2153−2160.

(2) Dumontet, C.; Jordan, M. A. Microtubule-binding agents: a dynamic field of cancer therapeutics. *Nature Rev. Drug. Discovery* **2010**, *9*, 790−803.

(3) Risinger, A. L.; Giles, F. J.; Mooberry, S. L. Microtubule dynamics as a target in oncology. *Cancer Treat. Rev.* **2008**, *35*, 255−261.

(4) Chen, S.-M.; Meng, L.-H.; Ding, J. New microtubule-inhibiting anticancer agents. *Expert Opin. Invest. Drugs* **2010**, *3*, 329−343.

(5) Pettit, G. R.; Singh, S. B.; Hamel, E.; Lin, C. M.; Alberts, D. S.; Garcia-Kendall, D. Isolation and structure of the strong cell growth and tubulin inhibitor combretastatin A-4. *Experientia* **1989**, *45*, 209−211.

(6) Lin, C. M.; Ho, H. H.; Pettit, G. R.; Hamel, E. Antimitotic natural products combretastatin A-4 and combretastatin A-2: studies on the mechanism of their inhibition of the binding of colchicine to tubulin. *Biochemistry* **1989**, *28*, 6984−6991.

(7) Pettit, G. R.; Temple, C., Jr.; Narayanan, V. L.; Varma, R.; Boyd, M. R.; Rener, G. A.; Bansal, N. Antineoplastic agents 322. Synthesis of combretastatin A-4 prodrugs. *Anti-Cancer Drug Des.* **1995**, *10*, 299−309.

(8) (a) Zweifel, M.; Jayson, G. C.; Reed, N. S.; Osborne, R.; Hassan, B.; Ledermann, J.; Shreeves, G.; Poupard, L.; Lu, S. P.; Balkissoon, J.; Chaplin, D. J.; Rustin, G. J. S. Phase II trial of combretastatin A4 phosphate, carboplatin, and paclitaxel in patients with platinum resistant ovarian cancer. *Ann. Oncol.* **2011**, *22*, 2036−2041. (b) Rustin, G. J.; Shreeves, G.; Nathan, P. D.; Gaya, A.; Ganesan, T. S.; Wang, D.; Boxall, J.; Poupard, L.; Chaplin, D. J.; Stratford, M. R. L.; Balkissoon, J.; Zweifel, M. A Phase Ib trial of CA-4P (combretastatin A-4 phosphate), carboplatin, and paclitaxel in patients with advanced cancer. *Br. J. Cancer* **2010**, *102*, 1355−1360.

(9) Siemann, D. W.; Chaplin, D. J.; Walike, P. A. A review and update of the current status of the vasculature-disabling agent combretastatin-A4 phosphate (CA4P). *Expert Opin. Invest. Drugs* **2009**, *18*, 189−197.

(10) Romagnoli, R.; Baraldi, P. G.; Carrion, M. D.; Cruz-Lopez, O.; Lopez-Cara, C.; Basso, G.; Viola, G.; Khedr, M.; Balzarini, J.;

Mahboobi, S.; Sellmer, A.; Brancale, A.; Hamel, E. 2-Arylamino-4-amino-5-aroylthiazoles. "One-pot" synthesis and biological evaluation of a new class of inhibitors of tubulin polymerization. *J. Med. Chem.* **2009**, *52*, 5551−5555.

(11) (a) Moreira Lima, L.; Barreiro, E. J. Bioisosterism: a useful strategy for molecular modification and drug design. *Curr. Med. Chem.* **2005**, *12*, 23−49. (b) Shan, Y.; Zhang, J.; Liu, Z.; Wang, M.; Dong, Y. Developments of combretastatin A-4 derivatives as anticancer agents. *Curr. Med. Chem.* **2011**, *18*, 523−538.

(12) Lange, J. H. M.; van Stuivenberg, H. H.; Coolen, H. K. A. C.; Adolfs, T. J. P.; McCreary, A. C.; Keizer, H. G.; Wals, H. C.; Veerman, W.; Borst, A. J. M.; de Looff, W.; Verveer, P. C.; Kruse, C. G. Bioisosteric replacements of the pyrazole moiety of rimonabant: synthesis, biological properties, and molecular modeling investigations of thiazoles, triazoles, and imidazoles as potent and selective CB1 cannabinoid receptor antagonists. *J. Med. Chem.* **2005**, *48*, 1823−1838.

(13) For anticancer molecules based on the 1,2,4-triazole ring see: (a) Zhang, Q.; Peng, Y.; Wang, X. I.; Keeman, S. M.; Aurora, S.; Welsh, W. J. Highly potent triazole-based tubulin polymerization inhibitors. *J. Med. Chem.* **2007**, *50*, 749−754. (b) Romagnoli, R.; Baraldi, P. G.; Cruz-Lopez, O.; Lopez-Cara, C.; Carrion, M. D.; Brancale, A.; Hamel, E.; Chen, L.; Bortolozzi, R.; Basso, G.; Viola, G. Synthesis and antitumor activity of 1,5-disubstituted 1,2,4-triazoles as *cis*-restricted combretastatin analogs. *J. Med. Chem.* **2010**, *53*, 4248−4258. (c) Ouyang, X.; Chen, X.; Piatnitski, E. L.; Kiselyov, A. S.; He, H.-Y.; Mao, Y.; Pattaropong, V.; Yu, Y.; Kim, K. H.; Kincaid, J.; Smith, L., II; Wong, W. C.; Lee, S. P.; Milligan, D. L.; Malikzay, A.; Fleming, J.; Gerlak, J.; Deevi, D.; Doody, J. F.; Chiang, H.-H.; Patel, S. N.; Wang, Y.; Rolser, R. L.; Kussie, P.; Labelle, M.; Tuma, M. C. Synthesis and structure−activity relationships of 1,2,4-triazoles as a novel class of potent tubulin polymerization inhibitors. *Bioorg. Med. Chem. Lett.* **2005**, *15*, 5154−5158. (d) Ohsumi, K.; Hatanaka, T.; Fujita, K.; Nakagawa, R.; Fukuda, Y.; Nihai, Y.; Suga, Y.; Morinaga, Y.; Akiyama, Y.; Tsuji, T. Synthesis and antitumor activity of *cis*-restricted combretastatins 5-membered heterocyclic analogues. *Bioorg. Med. Chem. Lett.* **1988**, *8*, 3153−3158. (e) Shi, Y.-J.; Song, X.-J.; Li, X.; Ye, T.-H.; Xiong, Y.; Yu, L.-T. Synthesis and biological evaluation of 1,2,4-triazole and 1,3,4-thiadiazole derivatives as potential cytotoxic agents. *Chem. Pharm. Bull.* **2013**, *61*, 1099−1104. (f) Singha, T.; Singh, J.; Naskar, A.; Ghosh, T.; Mondal, A.; Kundu, M.; Harwansh, R. K.; Maity, T. K. Synthesis and evaluation of antiproliferative activity of 1,2,4-triazole derivatives against EAC bearing mice model. *Ind. J. Pharm. Edu. Res.* **2012**, *46*, 346−351. (g) Li, X.; li, X.-Q.; Liu, H.-M.; Zhou, X.-Z.; Shao, Z.-H. Synthesis and evaluation of antitumor activities of novel chiral 1,2,4-triazole Schiff bases bearing γ-butenolide moiety. *Org. Med. Chem. Lett.* **2012**, *2*, 26−31.

(14) (a) Gaukroger, K.; Hadfield, J. A.; Lawrence, N. J.; Nlan, S.; McGown, A. T. Structural requirements for the interaction of combretastatins with tubulin: how important is the trimethoxy unit? *Org. Biomol. Chem.* **2003**, *1*, 3033−3037. (b) Cushman, M.; Nagarathnam, D.; Gopal, D.; He, H.-M.; Lin, C. M.; Hamel, E. Synthesis and evaluation of analogues of (*Z*)-1-(4-methoxyphenyl)-2-(3,4,5-trimethoxyphenyl)ethene as potential cytotoxic and antimitotic agents. *J. Med. Chem.* **1992**, *35*, 2293−2306.

(15) Thomae, D.; Perspicace, E.; Hesse, S.; Kirsch, G.; Seck, P. Synthesis of substituted [1,3]thiazolo[4,5-*d*][1,2.3]triazines. *Tetrahedron* **2008**, *64*, 9306−9314.

(16) Webb, R. L.; Eggleston, D. S.; Labaw, C. S.; Lewis, J. J.; Wert, K. Diphenyl cyancarbonimidate and dichlorodiphenoxymethane as synthons for the construction of heterocyclic systems of medicinal interest. *J. Heterocycl. Chem.* **1987**, *24*, 275−278.

(17) Szakács, G.; Paterson, J. K.; Ludwig, J. A.; Booth-Genthe, C.; Gottesman, M. M. Targeting multidrug resistance in cancer. *Nature Rev. Drug Discovery* **2006**, *5*, 219−234.

(18) Baguley, B. C. Multidrug resistance mechanism in cancer. *Mol. Biotechnol.* **2010**, *46*, 308−316.

(19) Toffoli, G.; Viel, A.; Tumiotto, I.; Biscontin, G.; Rossi, G.; Boiocchi, M. Pleiotropic-resistant phenotype is a multifactorial phenomenon in human colon carcinoma cell lines. *Br. J. Cancer* **1991**, *63*, 51−56.

(20) Dupuis, M.; Flego, M.; Molinari, A.; Cianfriglia, M. Saquinavir induces stable and functional expression of the multidrug transporter P-glycoprotein in human CD4 T-lymphoblastoid CEM rev cells. *HIV Med.* **2003**, *4*, 338−345.

(21) Clarke, P. R.; Allan, L. A. Cell-cycle control in the face of damage—a matter of life or death. *Trends Cell Biol.* **2009**, *19*, 89−98.

(22) Mollinedo, F.; Gajate, C. Microtubules, microtubule-interfering agents and apoptosis. *Apoptosis* **2003**, *8*, 413−450.

(23) Ganem, N. J.; Pellman, D. Linking abnormal mitosis to the acquisition of DNA damage. *J. Cell Biol.* **2012**, *199*, 871−881.

(24) Orth, J. D.; Loewer, A.; Lahav, G.; Mitchison, T. J. Prolonged mitotic arrest triggers partial activation of apoptosis, resulting in DNA damage and p53 induction. *Mol. Biol. Cell* **2012**, *23*, 567−576.

(25) Fernandez-Capetillo, O.; Lee, A.; Nussenzweig, M.; Nussenzweig, A. H2AX: the histone guardian of the genome. *DNA Repair* **2004**, *3*, 959−967.

(26) Weiss, R. H. p21Waf1/Cip1 as a therapeutic target in breast and other cancers. *Cancer Cell* **2003**, *4*, 425−429.

(27) Vermes, I.; Haanen, C.; Steffens-Nakken, H.; Reutelingsperger, C. A novel assay for apoptosis. Flow cytometric detection of phosphatidylserine expression on early apoptotic cells using fluorescein labelled annexin V. *J. Immunol. Methods* **1995**, *184*, 39−51.

(28) Baeriswyl, V.; Christofori, G. The angiogenic switch in carcinogenesis. *Semin. Cancer Biol.* **2009**, *19*, 329−337.

(29) Siemann, D.; Bibby, M.; Dark, G. Differentiation and definition of vascular-targeted therapies. *Clin. Cancer Res.* **2005**, *2*, 416−420.

(30) Kanthou, C.; Tozer, G. M. The tumor vascular targeting agent combretastatin A-4-phosphate induces reorganization of the actin cytoskeleton and early membrane blebbing in human endothelial cells. *Blood* **2002**, *99*, 2060−2069.

(31) Bergers, G.; Benjamin, L. E. Tumorigenesis and the angiogenic switch. *Nature Rev. Cancer.* **2003**, *3*, 401−410.

(32) Guidolin, D.; Vacca, A.; Nussdorfer, G. G.; Ribatti, D. A new image analysis method based on topological and fractal parameters to evaluate the angiostatic activity of docetaxel by using the Matrigel assay in vitro. *Microvasc. Res.* **2004**, *67*, 117−124.

(33) Porcù, E.; Viola, G.; Bortolozzi, R.; Mitola, S.; Ronca, R.; Presta, M.; Persano, L.; Romagnoli, R.; Baraldi, P. G.; Basso, G. TR-644 a novel potent tubulin binding agent induces impairment of endothelial cells function and inhibits angiogenesis. *Angiogenesis* **2013**, *16*, 647−662.

(34) Gasparotto, V.; Castagliuolo, I.; Chiarelotto, G.; Pezzi, V.; Montanaro, D.; Brun, P.; Palù, G.; Viola, G.; Ferlin, M. G. Synthesis and biological activity of 7-phenyl-6,9-dihydro-3*H*-pyrrolo[3,2-*f*]-quinolin-9-ones: a new class of antimitotic agents devoid of aromatase activity. *J. Med. Chem.* **2006**, *49*, 1910−1915.

(35) Altomare, A.; Burla, M. C.; Camalli, M.; Cascarano, G.; Giacovazzo, C.; Guagliardi, A.; Moliterni, A. G.; Polidori, G.; Spagna, R. *SIR97*: a new tool for crystal structure determination and refinement. *J. Appl. Crystallogr.* **1999**, *32*, 115−121.

(36) Sheldrick, G. M. SHELXL-97, *Program for Refinement of Crystal Structures*; University of Göttingen: Gottingen, Germany, 1997.

(37) Romagnoli, R.; Baraldi, P. G.; Kimatrai Salvador, M.; Brancale, A.; Fu, X.-H.; Li, J.; Zhang, S.-Z.; Hamel, E.; Bortolozzi, R.; Basso, G.; Viola, G. Synthesis and evaluation of 1,5-disubstituted tetrazoles as rigid analogues of combretastatin A-4 with potent antiproliferative and antitumor activity. *J. Med. Chem.* **2012**, *55*, 475−488.

(38) (a) Hamel, E. Evaluation of antimitotic agents by quantitative comparisons of their effects on the polymerization of purified tubulin. *Cell Biochem. Biophys.* **2003**, *38*, 1−21. (b) Verdier-Pinard, P.; Lai, J.-Y.; Yoo, H.-D.; Yu, J.; Marquez, B.; Nagle, D. G.; Nambu, M.; White, J. D.; Falck, J. R.; Gerwick, W. H.; Day, B. W.; Hamel, E. Structure−activity analysis of the interaction of curacin A, the potent colchicine site antimitotic agent, with tubulin and effects of analogs on the growth of MCF-7 breast cancer cells. *Mol. Pharmacol.* **1998**, *53*, 62−67.

(39) Ravelli, R. B. G.; Gigant, B.; Curmi, P. A.; Jourdain, I.; Lachkar, S.; Sobel, A.; Knossow, M. Insight into tubulin regulation from a complex with colchicine and a stathmin-like domain. *Nature* **2004**, *428*, 198−202.
(40) *Molecular Operating Environment (MOE 2008.10)*; Chemical Computing Group, Inc.: Montreal, Quebec, Canada, 2008; http://www.chemcomp.com.
(41) Korb, O.; Stützle, T.; Exner, T. E. PLANTS: Application of ant colony optimization to structure-based drug design. In *Ant Colony Optimization and Swarm Intelligence, 5th International Workshop, ANTS 2006,* ; Dorigo, M., Gambardella, L. M., Birattari, M., Martinoli, A., Poli, R., Stützle, T., Eds.; Springer: Berlin, 2006; LNCS 4150, pp 247−258.
(42) Liang, C. C.; Park, A. Y.; Guan, J. L. In vitro scratch assay: a convenient and inexpensive method for analysis of cell migration in vitro. *Nature Protoc.* **2007**, *2*, 329−333.